1   **Snow interception modeling: Isolated observations have led to many land**

2   **surface models lacking appropriate temperature sensitivities**

3

4   Jessica D. Lundquist[1], Susan Dickerson-Lange[2], Ethan Gutmann[3], Tobias Jonas[4], Cassie

5   Lumbrazo[1], and Dylan Reynolds[1,4]

6

7   [1]Civil and Environmental Engineering, University of Washington, Seattle, WA, USA

8   [2]Natural Systems Design, Seattle, WA, USA

9   [3]National Center for Atmospheric Research, Boulder, CO, USA

10   [4]WSL Institute for Snow and Avalanche Research SLF, Davos Dorf, Switzerland

11

12   **Corresponding Author:** Jessica D. Lundquist, Civil and Environmental Engineering, University

13   of Washington, Box 352700, Seattle, WA 98195, jdlund@uw.edu

14

15   **Abstract**

16   When formulating a hydrologic model, scientists rely on parameterizations of multiple processes

17   based on field data, but literature review suggests that more frequently people select

18   parameterizations that were included in pre-existing models rather than re-evaluating the

19   underlying field experiments. Problems arise when limited field data exist, when "trusted"

20   approaches do not get reevaluated, and when sensitivities fundamentally change in different

21   environments. The physics and dynamics of snow interception by conifers is just such a case,

22   and it is critical to simulation of the water budget and surface albedo. The most commonly-used

23   interception parameterization is based on data from four trees from one site, but results from this

24   field study are not directly transferable to locations with relatively warmer winters, where the

25   dominant processes differ dramatically. Here, we combine a literature review with model

26   experiments to demonstrate needed improvements. Our results show that the choice of model

27   form and parameters can vary the fraction of snow lost through interception by as much as 30%.

28   In most simulation, the warming of mean winter temperatures from -7°C to 0°C reduces the

29   modeled fraction of snow under the canopy compared to the open, but the magnitude of

30   simulated decrease varies from about 10 to 40%. The range of results is even larger when

31   considering models that neglect the melting of in-canopy snow in higher-humidity environments

32 where canopy sublimation plays less of a role. Thus, we recommend that all models represent

33 canopy snowmelt and include representation of increased loading due to increased adhesion and

34 cohesion when temperatures rise from -3 to 0°C. In addition to model improvements, field

35 experiments across climates and forest types are needed to investigate how to best model the

36 combination of dynamically changing forest cover and snow cover to better understand and

37 predict changes to albedo and water supplies.

38

39 **Keywords**: forest, snow, modeling, interception, hydrology, albedo, vegetation, history

1. INTRODUCTION

Both forest cover and snow processes are changing globally at unprecedented rates (Adams et al., 2009; Allen, 2009; Bormann, Brown, Derksen, & Painter, 2018; Halofsky, Peterson, & Harvey, 2020). These changes, their interactions, and their impacts are critical components of any model of the terrestrial water balance and energy balance. Substantial research has demonstrated that modeling forest-snow interactions is complicated (Dickerson-Lange et al., 2017; Helbig et al., 2020; Rutter et al., 2009). However, global land surface model representations of canopy snow interception are currently based on observations from only two studies (Hedstrom & Pomeroy, 1998; Storck, 2000). Employing a larger literature review and an interception model, we propose how to improve process representation of accumulation, ablation, and unloading of snow in the forest canopy. These improvements are critical for models that span multiple climates (e.g., global, mountain, continental, maritime, and/or climate change applications), as many current parameterizations are not transferable in space or time.

Snow accumulation under forests compared to the open varies from 40% to nearly identical amounts, and these differences are the dominant drivers of net changes in snow accumulation and duration (Dickerson-Lange et al., 2017; Lundquist, Dickerson-Lange, Lutz, & Cristea, 2013), which leads to differences in total runoff, particularly in summer streamflow (Cristea, Lundquist, Loheide II, Lowry, & Moore, 2014; Sun et al., 2018). Interception dynamics vary widely with forest structure and regional climate, as well as between individual storms (Carlyle-Moses & Gash, 2011; Lundquist et al., 2013; Moeser, Stähli, & Jonas, 2015). However, given historic difficulty in measuring interception (Friesen, Lundquist, & Van Stan, 2015), current measurements and understanding are limited to a few locations representing a minority of forest structures and climatic settings.

Due to a lack of better information, parameterizations that have been validated in only one specific setting are being used in global models, while parameterizations from another setting can differ in even the sign of their response to temperature (Andreadis, Storck, & Lettenmaier, 2009; Clark et al., 2015; Hedstrom & Pomeroy, 1998). Hedstrom and Pomeroy (1998) formulated maximum snow interception per unit vegetation area decreasing with temperature, due to increased snow rebound and decreased tree-branch stiffness, while Andreadis et al. (2009) described it increasing rapidly as temperatures warm above -3°C, due to

71 increasing cohesiveness of snow at warmer temperatures (Figure 1b). While these two

72 parameterizations match at low temperatures, a well-calibrated model subjected to warmer

73 temperatures (e.g., for a climate sensitivity experiment) would show a different hydrologic

74 response: interception will vary by a factor of four depending on the model chosen, with

75 subsequent effects on snowpack and soil moisture. These two formulations are based on (Fig.

76 1d) branches clipped to a pole in the Rocky Mountains (Schmidt & Gluns, 1991) or (Figure 1e)

77 two Douglas Firs on weighing lysimeters in the Oregon Cascades (Storck, 2000) and provide the

78 basis for the majority of our models.

79   [Insert Figure 1]

80   Changes in land surface albedo are another important, yet poorly understood, feedback in

81 global climate variability. Variability in land surface albedo between CMIP5 climate models can

82 explain 40-50% of the spread in modeled warming over the northern hemisphere (Qu & Hall,

83 2014; Thackeray & Fletcher, 2016), and intercepted snow in the canopy affects albedo by ~24%

84 (Webster & Jonas, 2018). Model differences in how intercepted snow is removed from the

85 canopy play an important role in the energy balance (Thackeray, Fletcher, & Derksen, 2014) but

86 vary widely and may be a function of air temperature and wind speed (Roesch, Wild, Gilgen, &

87 Ohmura, 2001) or a constant rate, leading to exponential decay of canopy snow (Hedstrom and

88 Pomeroy, 1998).

89   Both snow stored under the canopy and land surface albedo matter to society, and

90 calculations of both are influenced strongly by how a model represents both the capacity of snow

91 to accumulate in the canopy and the rate, timing, and mechanism(s) of how that snow is removed

92 from the canopy. In addition to increasing albedo, the longer snow stays on the canopy, the

93 longer there is time for canopy snow to sublimate, which can result in about 20-50% of the

94 winter precipitation returning to the atmosphere (Lundberg & Halldin, 2001; Pomeroy &

95 Schmidt, 1993; Sexstone et al., 2018). Snow lasting longer in the canopy also has more time to

96 melt, resulting in liquid water that may not be stored in the underlying snowpack. Consequently,

97 outside of high wind environments (e.g., Revuelto, López-Moreno, Azorin-Molina, and Vicente-

98 Serrano (2015)), over most of the snow accumulation season in forested environments, canopy

99 interception is the primary driver of spatial variability of snow on the ground (Mazzotti et al.,

100 2019). Total seasonal snow in the canopy can be increased by either increasing interception

101   loading capacity, decreasing melt and drip rates of canopy snow, decreasing sublimation, or

102   decreasing unloading, requiring that these processes be examined together.

103   Here, we review the literature to explain the history and epistemology of snow interception

104   modeling (Section 2), including the origin and evolution of algorithms in current models and the

105   original observations on which they are based. We focus specifically on loading and unloading

106   in the context of weather and climate, leaving issues of forest structure as a subject for future

107   work. We re-examine the observational literature in a global context to assess which process

108   representations are most supported by field and laboratory data to provide recommendations and

109   key hypotheses for testing. We employ a simple model of interception at two sites with different

110   mean winter temperature and humidity (Section 3) to illustrate how model representations lead to

111   different estimates of snow accumulation under forest cover and, more importantly, to different

112   temperature sensitivities, to establish priorities regarding essential observations for validation

113   and needed model modifications to adequately represent responses to forest and climatic change

114   (Section 4). Finally, we outline a path forward for both observationalists and modelers to ensure

115   a more holistic approach to understanding and modeling combined forest-snow-climate change

116   (Section 5).

117

118   **2. HISTORY OF SNOW INTERCEPTION MODELING**

119   **2.1 Basic Formulations and Concepts**

120   Most models take a similar form for the basics of interception (Table 1). When snow falls from

121   the sky, some fraction of it is intercepted by the forest canopy, up to some maximum amount that

122   the given canopy can hold, while the remaining fraction falls to the ground below (Figure 1).

123   The snow in the canopy may sublimate or fall beneath or adjacent to the canopy. The canopy

124   snow may also melt, in which case it may evaporate, drip to the ground below, and/or lubricate

125   the remaining canopy snow so that some mixture of melted and solid snow falls to the ground

126   below. Key parameters involved in modeling these processes include interception efficiency, I_e

127   (the fraction of snowfall intercepted at each timestep), the maximum interception, I_{max}, the

128   sublimation rate, S, the melt rate of intercepted snow, M, and the unloading rate, U. In most

129   models, these are some function of leaf area index, LAI, and/or fractional forest cover, which

130   represent how much canopy cover is present. Some models explicitly represent the canopy

131   energy balance and phase changes within it, while others parameterize conceptually how snow

132 behaves within the canopy (Table 1). We focus here on interception efficiency, maximum

133 interception, sublimation, melt, and unloading, with canopy structure left as a subject for future

134 research.

135 [Insert Table 1]

136 **2.2 Model Family Trees**

137 While significant earlier work existed observing and quantifying snow interception (section 2.3),

138 Hedstrom and Pomeroy (1998), hereafter referred to as HP98, were arguably the first to develop

139 a coherent system of equations for modeling all of the processes involved and have influenced

140 many models developed in subsequent years. Here we review their work in the context of the

141 literature as a whole, highlighting parallel developments and diverging ideas.

142

143 *2.2.1   Interception*

144 HP98 defined the interception rate as a function asymptotically approaching zero as total

145 interception approaches I_{max},

146 $$dI_s/dt = (I_{max} - I_s)(1 - e^{-C_l P_s \Delta t / I_{max}})/\Delta t \qquad (1)$$

147 where I_s is the intercepted snow per unit area, I_{max} is the maximum possible intercepted snow, P_s

148 is snowfall, t is time, and C_l is the canopy leaf contact area per unit ground area. This function

149 stemmed from prior work by Satterlund and Haupt (1967), who weighed a Douglas-fir and a

150 western white pine sapling (each $\sim$ 4 m high) during two storms in northern Idaho, showing an

151 increase and then leveling off of intercepted snow amounts over the course of these storms.

152 Satturlund and Haupt presented a conceptual understanding that interception rates start low

153 (when there was no snow in the tree), increase as initial snowflakes bridge gaps between the

154 needles, and then decrease again as falling ice crystals bounce off and as branches bend

155 sufficiently for snow to fall off, essentially approaching the maximum interception capacity.

156 This representation is referred to as a sigmoidal efficiency curve.   Only the decrease in

157 efficiency as I_s approaches I_{max} was preserved in HP98's formulation, making it an exponential,

158 rather than sigmoidal, function. The maximum value was modeled as

159 $$I_{max} = \alpha(0.27 + 46/\rho_s)LAI \qquad (2)$$

160 where LAI is the leaf area index, α is recommended to be 6.6 and 5.9 km m^{-2} for pine and spruce

161 following (Schmidt & Gluns, 1991), and the fresh snow density in kg m^{-3} is estimated by

162 $$\rho_s = 67.92 + 51.25e^{(T_{air})/2.59} \ , \tag{3}$$

163 where T_{air} is air temperature (°C).

164   The hard-coded parameters (0.27 and 46) in equation 2 are based on fitting a curve to

165 snow interception on branches at the two study sites in Schmidt and Gluns (1991): Fraser

166 Experimental Forest, Colorado, USA, winter 1989, and Nelson, British Columbia, Canada,

167 winter 1990. At both locations, approximately 30-cm long branches of different tree species

168 (Engelmann spruce, subalpine fir, and lodgepole pine, Fig. 1d) were attached to a horizontal steel

169 rod about 1 m above the snow surface. After each storm period, the snow was shaken off each

170 branch and into a plastic bag, which was weighed. Total snowfall was estimated from what

171 accumulated on an adjacent snow board. Schmidt and Gluns (1991) mentioned greater cohesive

172 forces at temperatures between -3 and 0°C multiple times (discussed further below), but these

173 comments were not translated into equations or functional forms in HP98's model development,

174 likely because temperatures in this range would play a very minor role in the cold continental

175 climate of Saskatchewan, Canada.

176   The fresh snow density numbers (equation 3) are based on storm total snow board

177 measurements from the two sites in Schmidt and Gluns (1991, their Table 2), as well as from

178 observations from the Central Sierra Snow Laboratory in California (USACE, 1956) (their plate

179 8-1, their Fig. 4). Note that the observations were taken over storm-total time periods, which

180 varied in duration but were generally 6-hours or longer, while the model equation is typically

181 applied at hourly timesteps. Due to the complexity of processes witnessed, both studies report

182 the relationship as likely highly uncertain, and subsequent studies have found air temperature to

183 be a poor predictor of new snowfall density (e.g., Wayand, Clark, and Lundquist (2017), their

184 Fig. 7). These equations have gone on to be used in a number of land surface models (Table 1

185 and Fig. 2), including VISA (Niu & Yang, 2004), Noah-MP (Niu et al., 2011), CLM (Lawrence

186 et al., 2019), and CLASS (Bartlett, MacKay, & Verseghy, 2006; Bartlett & Verseghy, 2015).

187   The concept of a maximum interception load appears in all models (Table 1). The

188 sigmoidal form (Satterlund & Haupt, 1967), of slow initial interception rates that increase with

189 time, only reappears in a recent development of FSM (Essery, 2015), with application by Moeser

190 et al. (2015), but was later removed from FSM by Mazzotti, Essery, Webster, Malle, and Jonas

191 (2020). Additionally, the influence of temperature and snow cohesion on interception, while

192 dropped in HP98, reappeared in an independent line of snow model development (Figures 1b and

193   2), described in Andreadis et al. (2009) and utilized in the VIC and DHSVM models. Their basic

194   interception model is based on two winters in the Oregon Cascades, where two full sized

195   Douglas Firs were weighed on load cells (Storck 2000, Fig. 1d). Temperatures at this site

196   hovered near 0°C all winter, but Storck (2000) noted that during one cold storm when

197   temperatures were less than -5°C, the maximum interception decreased by a factor of 4.

198   Andreadis et al. (2009) combined this observation with the results of Kobayashi (1987), who

199   found that between -3 and 0°C, the cohesion of ice increases, leading to increased interception on

200   boards. Thus, they modeled the maximum snow interception as increasing linearly between -3

201   and 0°C by a factor of 4.

202   To summarize, interception processes in almost all current land surface models can be traced

203   back to the evolution of interception efficiency in two storms in Idaho, which helped inform

204   equation (1) in HP98. The value of I_{max} in these models was determined by the behavior of

205   branches attached to a steel rod, or by comparing one cold interception event to average

206   conditions in Oregon combined with a study on boards, with the decision between the two

207   approaches depending primarily on which specific research groups and other modeling papers a

208   given model stemmed from (Figure 1 and Figure 2). While the originating studies all examined

209   evergreen conifers in mountains, the two study areas had very different climates (maritime vs.

210   continental), with different temperature regimes.

211   [Insert Figure 2]

212

213   *2.2.2   Unloading*

214   While maximum snow accumulation in interception models follows either HP98 or Storck 2000

215   (Figure 2), representations of unloading of canopy snow are more varied (Figure 3). Given their

216   differing foci on relatively cold (HP98) and warm (Storck 2000) environments, HP98 described

217   snow unloading from a tree as an exponential function of time, approaching zero over a few

218   days, while Storck (2000) observed frequent unloading whenever temperatures rose above zero.

219   Illustrated on the right side of Figure 3, Storck, Lettenmaier, and Bolton (2002) quantified the

220   ratio of solid snow mass release to meltwater drip to be 0.4, and this formulation was

221   incorporated by Essery et al. (2003) in JULES and by Andreadis et al. (2009) in VIC and

222   DHSVM. Pomeroy's further development of the HP98 model in CRHM added an additional

223   term, based on work by Gelfan, Pomeroy, and Kuchment (2004), wherein all snow was unloaded

224   from the canopy in solid form when ice-bulb temperatures remained above freezing for 3 hours

225   in the presence of wind speed greater then 0.5 m s^{-1}, but not all models using the equations of

226   HP98 added this modification (Fig. 3). A third line of reasoning originated with Roesch et al.

227   (2001), who were trying to improve albedo representations over the boreal forest in the

228   ECHAM4 GCM and disagreed with the premise of HP98 that intercepted snow would approach

229   zero simply as a function of time. Drawing on four observational studies with general

230   descriptions of how snow unloads at higher wind speeds and at temperatures greater than -3°C,

231   they formulated unloading to be a fraction of the existing intercepted snow, with the fraction

232   varying with the observed wind speed and canopy air temperature relative to threshold values.

233   These functions were adopted by multiple land surface models in the years following, including

234   VISA (Niu and Yang 2004), Noah MP (Niu et al. 2011), and CLASS (Bartlett and Veresghy

235   2015), as well as in the migration of CLM4.5 to CLM5.0 (Lawrence et al., 2019; Perket, 2015),

236   (Fig. 3). Liston and Elder (2006), in developing SnowModel, unloaded snow as a function of air

237   temperatures greater than 0°C but did not include wind-related unloading. Mazzotti, Essery,

238   Moeser, and Jonas (2020), in FSM2, implemented exponential decay unloading as in HP98, but

239   with different time constants for cold vs. melting snow conditions. Note that model decisions

240   about whether to calculate canopy snowmelt (and subsequent meltwater drip) appear to be made

241   independently of decisions about snow unloading (Fig. 3, Table 1), with the exception of models

242   deriving from Storck et al. (2002), which directly relate solid snow unloading with dripping melt

243   water.

244   [Insert Figure 3]

245   *2.2.3   Sublimation*

246   Due to greater winds and solar exposure, as well as larger exposed snow surface area,

247   sublimation from the canopy is larger than sublimation from the forest floor. Because canopy

248   sublimation only occurs when snow is in the canopy, total sublimation is directly linked to the

249   duration snow stays in the canopy. In all land surface models and most snow models,

250   sublimation increases with increasing wind speed and with decreasing atmospheric humidity

251   (Table 1). Wind speed is scaled as a function of canopy height, using either exponential or

252   logarithmic profiles. Two general families of formulas exist (Table 1). In CRHM, SnowModel,

253   and AMUDSEN, sublimation is calculated based on laboratory experiments (Thorpe & Mason,

254   1966), which related the sublimation rate of individual ice spheres to relative humidity and wind

9

255 speed. This is then modified to include the additional influence of solar radiation absorbed by

256 the particle as developed for a blowing snow model (Schmidt, 1972), and scaled based on

257 studying snow on an artificial tree (Schmidt, 1991) and a fractal analysis of photographs of snow

258 on boreal forest branches (Pomeroy & Schmidt, 1993). In most land surface models, the

259 formulas used for sublimation closely follow the model's representation of canopy evaporation.

260 VISA, CLASS, UEB, VIC, DHSVM, SUMMA, CLM, JULES, Noah-MP, and the latest version

261 of FSM all calculate sublimation based on bulk aerodynamic formula.   While models adjust for

262 stability conditions differently, see Lapo, Nijssen, and Lundquist (2019) for review, sublimation

263 scales with wind speed and with vapor pressure gradients in all but the rare representations of

264 stable conditions shutting down turbulence completely. We leave a full analysis of canopy wind

265 speed variations and stability corrections as a subject for future research.

266

267 **2.3   Recommendations Based on Published Observations**

268 Measurements of canopy snow interception are difficult (see Friesen et al. (2015) for a review of

269 techniques), but many more direct measurements exist than appear to have been used in model

270 development. Here, we review these observations to determine in which aspects they agree with

271 current modeling practices for interception and unloading, and in which aspects they suggest

272 changes are necessary.

273

274 *2.3.1   Interception efficiency*

275 Interception efficiency reaching 0 when total interception approaches a specific I_{max} is not

276 supported from collective observational evidence. Satterlund and Haupt (1967) originated the

277 idea of sigmoidal interception efficiency with time, reaching a maximum interception value.

278 This function was based on earlier work on the interception of liquid precipitation (Merriam,

279 1960). After hanging and weighing two 4 m high saplings (Douglas Fir and White Pine) for one

280 month in Priest River, Idaho in a clearing sheltered from the wind, their data showed that after

281 snow initially fell on the tree, the interception rate increased rapidly and then leveled off (Figure

282 4a). They described the leveling off as the capacity of the tree to retain snow.

283   [Insert Figure 4]

284

285   While most models include the idea that interception efficiency approaches zero as a
286   maximum interception value is approached, no published dataset other than Satterlund and
287   Haupt's examining conifers fits this form better than it would fit a constant interception
288   efficiency (Figure 4). Often only one or a few data points that appear to indicate a maximum
289   interception are used to justify the maximum. Data from both Switzerland and France (Helbig et
290   al., 2020), their Figure 5, show near constant interception efficiency over a range of snowfall
291   amounts. The exception is Moeser et al. (2015), who showed an initially increasing and then
292   decreasing interception efficiency over 9 storms in Switzerland. Observations from the
293   Nothofagus forests of the Southern Andes (Huerta, Molotch, & McPhee, 2019) suggest that the
294   models of both Hedstrom and Pomeroy (1998) and Moeser et al. (2016) consistently
295   underestimated the largest interception events, which would indicate their decrease in
296   interception efficiency was not supported in the Nothofagus forests.
297   Separately, observations in Japan show accumulated snow depth on boards of different
298   widths flattens out only for the heaviest snowfall and not for cases of moderate snowfall (Shidei,
299   1952) (translation can be found on page 119, Fig. 7.21 in Bunnell, McNay, and Shank (1985)).
300   Using spatial measurements in Hokkaido, Japan, Lundberg, Nakai, Thunehed, and Halldin
301   (2004) found that the snowfall fraction intercepted and lost to sublimation varied strongly with
302   forest sky view fraction but had no relationship with snowfall magnitude.
303   Throughout the literature, the raw data present a question: Is there a stable maximum
304   interception capacity which influences interception efficiency? The presence of a stable
305   maximum interception amount, pervasive in our modeling, may not be the best fit for the data
306   available (Fig. 4b-f). The discrepancy may be due, at least in part, to the difference between a
307   canopy system, which often has multiple layers of branches, including those overlapping from
308   adjacent trees, and an isolated hung sapling, or to the aggregation of multiple storms vs. a
309   presentation from one specific storm sequence. It could be due to a belief that there ought to be a
310   maximum carrying capacity, irrespective of whether there is evidence in the available data, or to
311   the true carrying capacity being so large (e.g., the point where a tree breaks) that measuring it is
312   impractical. Another explanation could be that the apparent maximum is reached when
313   unloading rates equal interception rates, although this equilibrium would likely be quite variable
314   between trees, storms, etc. A final consideration is how different functional forms of this
315   equation affect model stability. We explore these questions further in Section 3.

316

2.3.2 *Changing snow cohesion and adhesion*

Changing snow cohesion and adhesion with temperature is a well-documented physical process. The efficiency of snow interception is a function of adhesion and cohesion countered by elastic rebound. The cohesion between snow crystals increases between the temperatures of -3 and 0°C, and this increased cohesion increases snow interception (Bunnell et al., 1985). The angle of repose of a pile of snow crystals increases rapidly at temperatures above -3.5°C, approaching nearly vertical at temperatures near 0°C (Kuroiwa, 1967). Increased interception with warming temperatures has been observed on boards (Kobayashi, 1987; Pfister & Schneebeli, 1999; Shidei, 1952), when weighing trees (Shidei, 1952; Storck, 2000) and through comparing snow accumulation under trees and nearby clearings after storms (Dickerson-Lange et al., 2017; Roth & Nolin). Quasi-liquid layers are apparent on ice at temperatures slightly below 0°C (Sazaki, Zepeda, Nakatsubo, Yokomine, & Furukawa, 2012), and these facilitate increased growth rates of bonds between snow crystals. Any sequence of events leading to a thin film of water present on the trees or previously-intercepted snow before snow falls leads to the greatest adhesion and hence, the greatest interception efficiency (Bunnell et al., 1985; Shidei, 1952).

Schmidt and Gluns (1991) found that elastic rebound, i.e., bouncing, is greater for snow with higher specific gravity, but they also wrote, "Greater specific gravity is associated most often with warm storms, where cohesive forces reduce elastic rebound." Similarly, Filhol and Sturm (2019) found that colder crystals bounced more, but that crystal type mattered as well as temperature. In general crystal type is also a function of air temperature (Libbrecht, 2019; Nakaya, 1954). At temperatures between -3 and 0°C, snow crystals generally form dendrites and plates, which adhere and form aggregates more readily than needles and columns, which form at temperatures between -10 and -3°C (Nakaya, 1954). Below -10°C, dendrites form again, but at these colder temperatures, cohesion is much less (Nakaya, 1954). The total range of solid precipitation types possible at temperatures near 0°C, from crystals to ice pellets to freezing rain, is diverse and complex (Stewart, Thériault, & Henson, 2015). Even HP98, whose functional form of I_{max} (Figure 1) indicates the opposite, noted, "There is a slight trend for greater interception efficiency at higher temperatures."

To summarize, all of our physical understanding and empirical evidence indicates that the air temperature during snowfall is a predicting variable of the efficiency at which snow is

347   intercepted by the canopy. To a first order, some representation of increased interception

348   efficiency with temperatures rising between -3 and 0°C, should be included in all land surface

349   models. To further improve, some representation of the impact of temperatures prior to storm on

350   the canopy (cold versus warm enough to have a thin film of liquid water), as well as the cloud

351   physics and meteorology leading to the crystal type, could be included. However, using the

352   concept of I_{max}, which in some models changes with temperature (Figure 1), may not be the best

353   approach, as examined in Section 3.

354

355   ### 2.3.3   Snow unloading

356   Wind and warmer temperatures control the rate and timing of unloading snow and should be

357   included in modeling. Despite its use in many models, no observational data are presented in the

358   literature that support snow unloading as predominantly an exponential decay function of time.

359   This functional form may be used as a proxy for other processes but has no empirical or physical

360   basis. Rather, the literature supports wind removing 33-100% of the snow load in cases of dry

361   and cold snow without near-melt layers to bond it (Bunnell et al., 1985; Goodell, 1959; Hoover

362   & Charles, 1967); in many cases, wind also limits the net amount of snow intercepted during

363   colder storms, likely due to unloading happening simultaneously with interception. The effect of

364   wind on decreasing interception is greater when branches (or boards, as tested) are at steeper

365   angles (Shidei, 1952).

366   Rainfall and temperatures warming above 0°C are also common causes of snow

367   unloading. Satterlund and Haupt (1970) report that most frequently snow was "washed off of the

368   trees by rain." While the correlation in timing of warm temperatures and unloading is frequently

369   reported in the literature and is represented in the majority of models (Table 1 and Figure 3),

370   many models do not calculate melt for intercepted snow in the canopy. Thus, many unload all

371   snow in a solid form, even at air temperatures greater than 0°C. Quantifying how much

372   intercepted snow is unloaded as solid snow versus meltwater is difficult, and reports range from

373   drip being "uncommon" in California (Kittredge, 1953) to "constant" in Oregon (Miller, 1962).

374   Satturlund and Haupt (1970) stated that only 5% of the intercepted snow became liquid

375   meltwater drip. Miller (1966) postulated that the "the release of intercepted snow occurs after

376   20% of it has melted" based on examination of the timing and likely energy input to snow

377   observed by studies weighing a tree in Japan (Shidei, 1952). Storck (2000) derived the

13

378 conclusion that 40% of liquid meltwater drip falls as solid snow based on careful comparisons of

379 adjacent lysimeter readings in the open and under the forest during two different 2-week periods

380 in December of each year when there was neither rain nor melting of ground snow. Storck

381 (2000) advised that the consistency of a 40% ratio across only two carefully-chosen study

382 periods was more of a hypothesis to be further tested than a conclusive value. Thus, while

383 energy available for melt, e.g., warmer temperatures, is clearly associated with unloading, the

384 form (solid or liquid) of that unloaded water is less clear. Unloaded solid snow adds mass to the

385 underlying snowpack, while unloaded liquid water may refreeze in the underlying snowpack, be

386 retained as liquid water in the underlying snowpack, or pass through the snow to contribute

387 immediately to soil moisture and/or runoff.

388

389 **3   METHODS: FORMULATING IMODEL**

390 To better understand which model parameters and processes have the largest impact on model

391 output, we investigate how different model interception configurations impact both snow

392 accumulation under the canopy and snow duration in the canopy. Because the duration snow

393 stays in the canopy impacts the likelihood that intercepted snow will sublimate or melt, and

394 hence not contribute to accumulation, these processes are closely linked.

395   While all existing models have a maximum interception parameter, the collective data

396 supporting this is not clear (Section 2.c.i). Also, while interception efficiency should increase

397 with temperature (Section 2.c.ii), incorporating this may not make a large difference in model

398 performance, particularly if unloading depends on temperature. For example, Niu et al. (2011)

399 illustrated Noah-MP simulations that match the dataset from Storck (2000) well, despite using

400 formulations primarily derived from HP98 (Figure 2).

401   To determine which model choices have the greatest impact on model results, we

402 formulate the experimental interception model, iModel, which has two state variables:

403 intercepted snow in the canopy (I_s) and snow under the canopy (SWE_u). The model can be

404 configured with a set maximum interception value (I_{max}), such that $I_e = f (I_s , I_{max})$, I_{max}

405 constant, or with a variable maximum interception value, $I_e = f (I_s , I_{max})$, $I_{max} = f(T_{air})$. For

406 both of these, the time evolution of intercepted snow is defined by

407

408 $$\frac{dI_S}{dt} = \left[(I_{max} - I_S)\left(1 - e^{-\left(\frac{P_S}{I_{max}}\right)}\right)\right] - S - I_s\left(M_T\frac{T_{air}}{C_T} + M_v\frac{U}{C_V} + M_{td}C_{td}\right) - M_{fac}T_{air} \quad (4)$$

409

410 where I_e is interception efficiency, P_s is snowfall, I_{max} is the maximum interception capacity, S is

411 sublimation rate, T_{air} is air temperature, U is wind speed, C_T and C_V are coefficients for rates of

412 unloading with temperature and wind, respectively, as in Roesch et al. (2001) and Niu et al.

413 (2011). C_{td} is the rate of exponential-decay unloading, as in Hedstrom and Pomeroy (1998), and

414 M_{fac} is the melt rate as a function of degrees C above 0°C. Each unloading formula has a

415 multiplier coefficient (M_T, M_v, M_{td}) so that the process may be turned off or rates may be

416 modified. The constant I_{max} is set the minimum value in Table 3, while the variable I_{max} scales

417 linearly between temperatures of -3 and 0°C, such that it equals the minimum value at -3°C or

418 lower temperatures and reaches the minimum plus the scale factor at 0°C (Table 3).

419   The sublimation rate is calculated as

420 $$S = C_{sub}U(e_{ss} - e_a) \quad (5)$$

421 where C_{sub} is a parameter, e_{ss} is the vapor pressure above the canopy snow, assumed to be the

422 saturation vapor pressure over ice at the smaller of air temperature or 0°C, and e_a is the

423 atmospheric vapor pressure, calculated as a function of air temperature and relative humidity

424 using the Magnus-Tetens formula (Murray, 1966) with coefficients from Alduchov and Eskridge

425 (1996), as described in Feld, Cristea, and Lundquist (2013).

426   The interception efficiency may also be configured without a maximum interception

427 value, with either a constant efficiency (I_e constant, no I_{max}), or an interception efficiency that

428 varies with temperature ($I_e = f(T_{air})$, no I_{max}). In this case the time evolution of intercepted snow

429 is decribed by:

430

431 $$\frac{dI_S}{dt} = I_eP_s - S - I_s\left(M_T\frac{T_{air}}{C_T} + M_v\frac{U}{C_V} + M_{td}C_{td}\right) - M_{fac}T_{air} \quad (6)$$

432

433 with variables and parameters defined the same as for (4). Thus, the model allows us to

434 investigate canopy loading configurations, with or without dependence on temperature or

435 maximum interception, while also testing their sensitivity to unloading rates and configurations,

436 through changing their multipliers.

15

437   Snow below the canopy accumulates as a function of snowfall that is not intercepted plus

438 unloaded solid snow from the canopy. Melt is not calculated for subcanopy snow. Liquid water

439 falling from the canopy is presumed to pass through the subcanopy snowpack without

440 contributing to subcanopy SWE. This is a fair assumption in warm maritime regions like the U.

441 S. Pacific Northwest, where frequent rain on snow results in a saturated and isothermal

442 snowpack with flow channels through it (Pflug, Liston, Nijssen, & Lundquist, 2019). However,

443 the model may underestimate subcanopy SWE in cases when a deep subcanopy snowpack stores

444 liquid water and may refreeze the water. We examine this in more detail in Section 5.2.

445   The model uses the Matlab ordinary differential equation solver, ode15s, which starts

446 with initial conditions of 0 snow in the canopy and then compares the results of first and fifth

447 order Runge-Kutta methods to determine the error and appropriate timestep (Shampine &

448 Reichelt, 1997). This approach allows for directly solving differential equations 4 and 6, given

449 the dependence of changes in intercepted snow on the snow currently in the canopy.

450   Atmospheric forcing data are drawn from 1997-1998 observations at Umpqua, Oregon,

451 described in Storck (2000) and from 2008-2009 observations at the Swamp Angel site at Senator

452 Beck, Colorado, described in Landry, Buck, Raleigh, and Clark (2014). The Oregon data include

453 2-hourly observations of precipitation, air temperature, relative humidity, and wind, as well as

454 weighing measurements of snow water equivalent (SWE) under the canopy, in the open, and in

455 three trees. This location is chosen because of its high-quality observations and warm winter

456 temperatures, to which we expect our model variations to be sensitive.   The Colorado data

457 include hourly observations of precipitation, air temperature, relative humidity, and wind, as well

458 as observations of snow in a forest clearing. The clearing SWE timeseries is a function of

459 combining continuous snow depth measurements with density from periodic snow pit

460 observations. This location was chosen as a colder and drier site for comparison of model

461 sensitivities to changing temperatures; however, note that there are no under-canopy snow

462 observations for this site. Mean values for the 1 December to 1 April period during each site's

463 analysis year are detailed in Table 2.

464   [Insert Table 2]

465   Model simulations were designed not to pick the best configuration but rather, to

466 illustrate the relative sensitivity to different model choices in two different environments.

467 Observations from Oregon were used to benchmark model performance and select reasonable

468   baseline model parameters from the literature (Table 3). Using this fixed set of parameters, we

469   examined the impact of changing the model's representation of loading and unloading on the

470   timeseries of cumulative snow water equivalent added to the subcanopy snowpack (Figure 5) and

471   the timeseries of intercepted snow in the canopy (Figure 6). We then examined the impact of

472   doubling ($2C_{sub}$) and halving ($0.5C_{sub}$) sublimation, not allowing snow to melt in the canopy

473   ($M_{fac} = 0$), and halving the rate of exponential unloading ($0.5M_{td}$), for each of the loading and

474   unloading schemes. These simulations were each repeated across a range of temperatures, by

475   uniformly increasing or decreasing air temperature to adjust the mean December to March

476   temperature to range from -7°C (which was observed at the Colorado site) to 0°C (which was

477   observed at the Oregon site). This range represents modeled snow evolution at colder or warmer

478   sites experiencing the same sequence of weather events, e.g., as might be expected at nearby

479   higher or lower elevations. In these scenarios, total precipitation and relative humidity are held

480   fixed, but the fraction of precipitation falling as snow and the vapor pressure are adjusted with

481   temperature. The modeled temperature sensitivity is compared to literature values.

482   [Insert Table 3]

483   For each simulation, the fraction of snow below the canopy compared to the open is

484   calculated as the ratio of total model snow accumulated over the season (subcanopy:open),

485   neglecting melt. The ground observations at the Oregon site, from a weighing lysimeter, were

486   also presented as the cumulative sum of positive changes in SWE, neglecting melt, following the

487   approach of Dickerson-Lange et al. (2017). The implications of neglecting melt are discussed

488   further in Section 5.2. The fraction of time snow is in the canopy is calculated as the total

489   timesteps with model intercepted snow greater than 0.5 mm divided by the total model timesteps

490   during the evaluation period. For Oregon, this period encompassed 18 November 1997 to 7

491   April 1998 (the duration of measurements), while for Colorado this period encompassed 1

492   October 2008 to 30 April 2009 (the duration of snowfall events).

493

494   **4   IMODEL RESULTS**

495

496   **4.1 Comparisons to timeseries of observational data**

497   With the baseline parameter set (Table 3), both temperature-based unloading and exponential-

498   decay unloading schemes were able to simulate below canopy snow accumulation (Figure 5a,b)

17

499   and intercepted snow (Figure 6a) close to observed values at Umpqua, Oregon. The loading

500   schemes with interception efficiency a function of air temperature (red and orange lines)

501   performed better with temperature-wind unloading (Figures 5a and 6a), while the loading

502   schemes with a constant I_{max} (blue lines) performed better with exponential decay unloading

503   (Figures 5b and 6a).   In Colorado, within canopy and subcanopy observations were not

504   available, but the same model configurations showed sensitivity to the different climate, with

505   snow under the canopy in Colorado accumulating about 65% of that in the open, compared to

506   only about 40% accumulating subcanopy in Oregon (Figure 5).

507   [Insert Figure 5]

508   At the Oregon site, the two simulations with loading dependent on air temperature grouped more

509   closely together, whereas at the Colorado site, the two simulations with I_{max} grouped more

510   closely together (Figure 5). In all cases, the simulations with I_e = constant, no I_{max} and with I_e =

511     $f(I_s , I_{max})$, $I_{max} = f(T_{air})$ fell close to or in between the other two loading schemes. Therefore,

512   for clarity in visualization, only simulations with $I_e = f(I_s , I_{max})$, I_{max} = constant and with I_e =

513     $f(T_{air})$, no I_{max} are shown in subsequent plots. In the interception timeseries for Colorado (Figure

514   6c), the temperature-dependent loading schemes were indistinguishable from those with no

515   temperature dependence because snow almost never fell in the -3 to 0°C temperature range

516   (Figure 6d).   The choice of loading scheme produced the largest variation in canopy SWE when

517   coupled with exponential-decay unloading (Figure 6c). At both locations, the model simulations

518   with I_{max} led to similar interception timeseries with both exponential and temperature-wind

519   unloading schemes, but over twice as much snow accumulated in the canopy when the

520   simulation with no I_{max} was coupled with the exponential unloading scheme (Figure 6a, c).

521   [Insert Figure 6]

522   Beyond different temperature regimes and sensitivities to loading schemes, the two sites

523   varied in the modeled fate of intercepted snow (Figure 7). The warm and moist Oregon site has

524   very little sublimation, as the relative humidity was close to 100% during times when snow was

525   in the canopy, but the amount of snow melting from the canopy was comparable with that

526   unloading. In contrast, the colder and drier Colorado site had comparable sublimation and

527   unloading from the canopy, with less snow melting. This affected the relative sensitivity of each

528   site to changing model parameter related to melt and sublimation, as discussed in the next

529   section.

530   [Insert Figure 7]

531

4.2 Model sensitivity to parameter change and temperature change

533   As illustrated with the timeseries (Figures 5 and 6), multiple model configurations can produce

534   similar results at a single site, with similar timing of snow in the canopy. However, the maritime

535   (OR) and continental (CO) sites had different fates of that intercepted snow (Figure 7) and

536   different fractions of snow accumulating beneath the canopy compared to the open (Figure 5).

537   To investigate the model's sensitivity to changing parameters and temperatures in these two

538   different climates, we ran the model at both sites with uniform temperature offsets ranging from -

539   7 to 0°C at the Oregon site and from 0°C to +7°C at the Colorado site, such that the weather

540   timeseries at each was adjusted towards the mean winter temperature at the other. The range of

541   parameters and loading/unloading schemes discussed in Section 3 illustrate a range of reasonable

542   results that might be expected from existing land surface models.   The results provide an

543   indication of the uncertainty in simulations performed at a given temperature and with perturbed

544   temperatures, which is one measure of model transferability.

545   For each simulation and mean December-March temperature, we consider the fraction of

546   snow water equivalent accumulating below the canopy compared to the open and the fraction of

547   time snow is in the tree (Figure 8). Observations at the Oregon site fell within the range of the

548   simulations that included canopy melt, but the simulations without canopy melt were far from

549   observations. At the Colorado site, simulations without melt fell within the range of those with

550   melt, indicating that this was a less sensitive model choice at this site.

551   [Insert Figure 8]

552   With mean Dec-Mar temperatures of -7°C, the relative amount of snow accumulating

553   below the canopy depends both on the time that snow stays in the canopy and the sublimation

554   rate, such that simulations with more time to sublimate and/or more rapid sublimation lose more

555   snow to the atmosphere, with the subcanopy:open snow accumulation ratio varying by up to

556   30%. At these temperatures, the lack of canopy snowmelt does not affect the fraction, since

557   temperatures are not warm enough to melt snow at times snow is in the canopy. The drier

558   Colorado site has greater sensitivity to modeled sublimation rates and thus a wider spread in

559   subcanopy snow fraction. As illustrated in Figure 7, a factor of two increase in sublimation at

560   the Colorado location would make total sublimation substantially more than unloading, whereas

19

561   a factor of two increase in sublimation in Oregon would still leave total sublimation less than

562   half of unloading. The fraction of time snow is present in the canopy varies up to 15% at either

563   site and is a function of the amount of loading and the combined rates of loss (to sublimation

564   and/or melt) and unloading.

565   As mean Dec-Mar temperatures approach 0°C, not only does the total snow on the

566   ground decrease, but the relative fraction of snow below the canopy compared to the open

567   decreases for most simulations (Figure 8 a,c), as has also been documented in the literature

568   (Dickerson-Lange et al. 2017; Roth and Nolin 2019).   Excluding the no-melt simulations, the

569   Oregon site was more sensitive to temperature change than the Colorado site (Figure 8), with

570   decreases in the ratio of snow subcanopy ranging from -17% to -39% (about a 20% range). In

571   contrast, for the Colorado simulations, the ratio of snow subcanopy decreased by -7% to -17%

572   (about a 10% range) with 7°C warming. The temperature sensitivity at the Colorado site was

573   driven by increases in sublimation, as the water vapor pressure gradient increased when air

574   temperatures warmed above 0°C, but the snow surface temperature was capped at 0°C. Thus,

575   while simulations with no canopy melt showed slightly less sensitivity to warming temperatures,

576   all model simulations at the Colorado site exhibited decreases in both relative snow below the

577   canopy and fraction of time snow is in the canopy. Because of the minimal amount of

578   sublimation at the maritime site (Figure 7), the climate sensitivity results from intercepted snow

579   melting and dripping instead of unloading in solid form. For these warm temperatures with an

580   isothermal subcanopy snowpack, drip results in a loss of water from the snow system.

581   Simulations without canopy melt were unable to represent these key processes.

582

583   **5   DISCUSSION**

584   **5.1 Model Sensitivities and Indications for Experimental Design**

585   The model simulations at Umpqua, OR and Senator Beck, CO illustrate both the relative order of

586   importance of model decisions for two locations and the importance of considering multiple

587   climates. In these simulations, the model decision with the greatest impact on model sensitivity

588   to temperature change was the choice to allow canopy snow to melt (Figures 8 and 9), which is

589   currently included in about half of land surface models (Figure 3; Table 1). However, this result

590   only appeared when modeling at the maritime site with mean winter temperatures near 0°C.

591   Colder and/or drier climates lose more snow to sublimation than to melt (Figure 7), and research

592 focused on these regions would not likely identify canopy melt as a process critical to hydrology.
593 However, forest cover is extensive in many maritime snow zones, such as the Pacific Northwest
594 of the U.S., the Coast Mountains of western Canada, and much of Japan, and these regions are
595 loci of some of the largest divergence in snow simulations across multi-model ensembles (R. S.
596 Kim et al., 2020). Given that most models are intended to simulate snow responses to changes in
597 weather and climate globally, appropriately representing canopy melt is essential.

598 The model choice with the greatest impact on the fraction of subcanopy snow
599 accumulation compared to the open at a specific mean winter temperature was the sublimation
600 rate (Figure 9), which had a greater impact in conjunction with the unloading scheme because
601 snow lasting longer in the canopy sublimated more. These impacts were much greater at the
602 drier Colorado site. Unlike canopy melt, which is a known process that could simply be added to
603 model code, sublimation is extremely difficult to measure, and the physics leading to variations
604 in sublimation rates, such as the influence of stability and wind fields through forests, are still an
605 active area of study and debate (LeMone et al., 2019).

606 The choice of model loading scheme was equally as important as the choice of model
607 unloading scheme (Figure 9), but the best choice of one was dependent on the choice of the other
608 (Figures 5 and 6). While comparing our model simulations to observations at one site was not
609 sufficient to declare any loading/unloading scheme superior, the literature review suggests that
610 temperature-based loading and unloading is supported by observations and physical
611 understanding. While the combination of loading to a fixed I_{max} and exponential unloading
612 matches observations well (Figures 5b and 6a), it may prove less transferable once more
613 observations are available.

614 Simulations employing loading schemes with interception efficiency a function of air
615 temperature had greater sensitivity to changing temperatures (Figure 9). This greater sensitivity
616 is supported by the literature. In the Pacific Northwest, a 3°C average winter temperature
617 increase across multiple sites corresponded with an observed 50% decrease in the under-
618 forest:open peak snow accumulation (Dickerson-Lange et al. 2017, their Fig. 3). A 40%
619 decrease in this ratio was observed between cold and warm storms which differed by ~6°C at
620 sites in Oregon (Roth and Nolin 2019, their Fig. 4). Over 30 years of observations in the boreal
621 forest of Northern Sweden showed that the ratio of snow under the forest compared to the open
622 has declined about 20% (Kozii, Laudon, Ottosson-Löfvenius, & Hasselquist, 2017). They found

623   that the best explanations for this variation were that the amount of precipitation falling at

624   temperatures less than -3°C led to more similar forest:open ratios, and that the number of total

625   days with temperatures above +0.4°C led to lower forest:open ratios. Thus, their work also

626   supports the conclusions here that interception efficiency increasing above -3°C, and melt and

627   sublimation losses increasing above 0°C, are important processes to represent in models to

628   adequately simulate sensitivity to temperature changes.

629

630   **5.2 Canopy melt, drip, and subcanopy snow**

631   As formulated, iModel does not add liquid melt water to the snow below the canopy, and thus,

632   whether the model simulates canopy snowmelt or simply unloads solid snow directly impacts the

633   subcanopy SWE accumulation. Meltwater from the canopy has been observed refreezing in the

634   snowpack in some environments (Teich et al., 2019), so by not allowing meltwater drip to add to

635   subcanopy SWE, iModel may be overestimating the hydrologic impact of melting canopy SWE.

636   However, the degree of this overestimation is a function of the environment, and the

637   assumption that melt water generally passes through the snowpack is fair at warm maritime sites

638   similar to the Oregon site simulated here. Sites with large oscillations in temperature, such as

639   periods of melt following periods with air temperatures substantially below 0°C, often have cold

640   and dry snowpacks that are capable of incorporating canopy melt through increasing residual

641   water content and/or refreezing. In contrast, warmer maritime sites frequently experience rain on

642   snow, resulting in saturated and isothermal snowpacks. Observations show that under these

643   conditions liquid water drains from the snowpack in less than a day, often at snowpack densities

644   less than would be assumed from observations in colder climates, leading to a lack of

645   transferability of some model representations of snowpack liquid water percolation (Pflug et al.,

646   2019). When analyzing errors in snow accumulation modeling in maritime regions, a significant

647   source of error arises from partitioning precipitation into rain vs. snow (Wayand et al., 2017;

648   Wayand, Stimberis, Zagrodnik, Mass, & Lundquist, 2016). The model choice to melt canopy

649   snow or unload it in solid form would similarly impact the model evolution of subcanopy SWE.

650   Here, we deliberately focused on subcanopy:open SWE accumulation ratios, neglecting

651   the influence of melt and not plotting actual SWE on the ground. Lundquist et al. (2013)

652   discussed the importance of midwinter melt in removing subcanopy snow in regions with warm

653   winters and plotted (their Figure 4) how the relative differences in subcanopy to open snow gain

654 vs. loss contributed to differences in peak SWE on the ground. For 1997-98 at Umpqua, Oregon,

655 the same data examined here, peak SWE on the ground was 222 mm in the open compared to 50

656 mm under the forest (Lundquist et al. 2013). Of this, 131 mm of the difference could be

657 attributed to accumulation differences, while only 52 mm could be attributed to melt differences,

658 with 11 mm of snow in the open lost during a period when no snow was on the ground under the

659 forest. These results suggested that while greater midwinter melt occurs under the canopy than

660 in the open, snow lost through interception processes accounts for a larger fraction of the

661 difference. Dickerson-Lange et al. (2017) followed up by examining paired observations of

662 snow in the forest and under canopies across the Pacific Northwest and found that throughout the

663 region, differences in snow accumulation explained the bulk of seasonal differences in both peak

664 SWE and snow duration. Given the high humidity and low sublimation in the maritime region,

665 the only way these observations can occur is for canopy snow to melt, and for the meltwater to

666 pass through the snow below the canopy, not contributing to subcanopy SWE accumulation.

667   Thus, we argue that all models should include canopy melt to accurately represent

668 subcanopy snow in warm maritime environments. Our results are not sufficient to argue the

669 importance of this representation in other environments, which may explain why the family tree

670 of models that include canopy melt (Figure 3) consists primarily of models that have included

671 the Oregon dataset in their evaluation.   In regions outside the maritime Pacific Northwest,

672 observations of snow stratigraphy and density in adjacent forest-covered and open areas show

673 that snow composition and the range of observed snow density under forests is clearly more

674 variable than in an adjacent opening (Teich et al., 2019). However, under-canopy snow is not

675 consistently more or less dense (Broxton, van Leeuwen, & Biederman, 2019), see their

676 supplemental material. Therefore, the fate of melting canopy snow and under-forest snow

677 evolution warrants further study.

678

679 **5.3 Order of operations, model stability and time-stepping schemes**

680 Often unloading happens during interception events, particularly in colder storms with high

681 winds or in warmer storms when snowfall changes to rain. While loading and unloading are two

682 separate processes, data often contain both, and models may solve an ordinary differential

683 equation (ODE) with adaptive timesteps and near-simultaneous adjustments of both loading and

684 unloading, as we have here, or may have a set order of operations, such that unloading may only

685   be allowed after an interception event. With this in mind, our concept that interception

686   efficiency decreases over time might simply be an effect of simultaneous unloading. There is

687   also a chance that within-storm unloading is accounted for twice in the model: first, by way of an

688   erroneously reduced interception efficiency, and again by way of the unloading function.

689   Numerical details are seldom reported in papers and are beyond the scope of this work.

690   However, we encourage anyone working on interception model development to pay particular

691   attention to the coding of the processes.

692

693   **5.4 Canopy Structure**

694   We have focused here on interception processes within a single tree or idealized canopy,

695   neglecting the impact of canopy structure. Our existing interception datasets also weigh single

696   trees or branches, and thus do not resolve canopy structure effects. However, moving forward, if

697   we plan to use snow on the ground as an evaluation dataset for interception modeling, we must

698   ensure that the evaluation is done in the context of a full energy and mass-balance model that

699   represents canopy structural effects on the domain over which measurements take place (e.g.,

700   Mazzotti, Essery, Webster, et al. (2020) and references therein). Beyond impacting snow on the

701   ground, the canopy arrangement will also affect interception processes. Canopy elements with

702   more solar exposure will lose intercepted snow first (either from sublimation or melting), and

703   canopy elements with more wind exposure may either intercept more snow (e.g., preferential

704   deposition of snowfall along downwind canopy edges or fog harvesting in riming conditions) or

705   lose snow more rapidly (from wind unloading).

706

707   **6   CONCLUSIONS**

708   Current global land surface representations of snow interception by forest canopies are based on

709   a handful of observations from two locations. However, despite the similar observational basis,

710   models vary in whether canopy loading capacity or efficiency increases with temperature, in

711   whether or not they model canopy snow melt, and in how they represent unloading. Based on

712   simulations varying these components, these differences lead to different estimates in how snow

713   accumulation under the canopy compares to the open and different sensitivities regarding how

714   snow in forested regions responds to changes in temperatures.

715   In the Northern Hemisphere winter, approximately 50% of the snow covered zone is
716   forested (E. Kim et al., 2017). However, most ground observations of snow are located in forest
717   clearings (Farnes, 1967), and current satellite remote sensing of snow cannot visibly see nor
718   reliably measure snow under forests (Rittger et al., 2020; Vuyovich, Jacobs, & Daly, 2014).
719   Therefore, snow under a forest canopy must be estimated or modeled relative to snow observed
720   in the open. Here, variations in interception processes alone led to subcanopy snow
721   accumulation ratios compared to the open that varied by 30%, suggesting that interception
722   processes contribute to a large component of uncertainty in modeling the current hydrology of
723   snow and forest-covered regions and in predicting the hydrologic response of these regions to
724   forest or temperature change.

725   The literature review and modeling presented here reveal that there are ways to better
726   constrain current model variations. Our analysis suggests, that, at a minimum, all model
727   representations of snow interception should model snow melt in the canopy to accurately
728   represent canopy effects in maritime regions. At the wet and warm Oregon location, simulations
729   without canopy snow melt showed the least sensitivity to temperature and were unable to match
730   observations of both snow in the canopy and snow beneath the canopy.

731   We further suggest that models should include a temperature-based representation of
732   increased cohesion as snow approaches the melting point, which increases the canopy
733   interception efficiency and/or capacity. Ample observational evidence demonstrates that snow
734   cohesion increases as temperatures approach the melting point, leading to greater interception
735   efficiency. Model simulations show that while any of the existing snow loading
736   parameterizations can match a season of intercepted snow data, those with interception
737   efficiency varying as a function of temperature show more sensitivity to temperature change,
738   more closely matching variations reported in the literature.

739   The choice of modeling changes in interception efficiency (I_e) directly or in maximum
740   interception efficiency (I_{max}, with I_e a function of I_{max}) led to differences in simulated snow, but
741   these differences were smaller than most other changes tested. Therefore, we recommend not
742   using I_{max} because it is an unnecessary model complication and is not supported in the literature
743   (Figure 4), but if it is already built into a model, it is less important to update than the
744   recommendations above. Similarly, either an exponential decay function or a physical basis for
745   snow unloading (e.g., temperature and wind dependence) could replicate observations from

746 Oregon. We recommend temperature and wind based unloading based on the observational
747 literature and strongly recommend that model loading and unloading schemes be examined
748 together and in the context of canopy sublimation and melt.
749   With the exception of a few studies (e.g., Hedstrom and Pomeroy 1998 and Storck 2000),
750 direct observations of snow interception have not been impressive in the years since the work in
751 Japan in the 1950s and 60s (Shidei, 1952). More locations, with a range of forest types and
752 climates, should be targeted for careful, detailed lysimeter and tree weighing work, accompanied
753 by accurate atmospheric data to run and test land surface models of snow evolution. Such work
754 should be accompanied by newer technology, such as time-lapse photography (Bartlett &
755 Verseghy, 2015) and lidar measurements of the forest (White et al., 2016) and the snow beside
756 and beneath it (Deems, Painter, & Finnegan, 2013). Constraining our estimates of snow under
757 forest canopy depends on model improvement, and the evaluation of canopy interception
758 processes and their representation is only possible with more observations.
759

771

772 **REFERENCES**
773 Adams, H. D., Guardiola-Claramonte, M., Barron-Gafford, G. A., Villegas, J. C., Breshears, D. D.,
774   Zou, C. B., . . . Huxman, T. E. (2009). Temperature sensitivity of drought-induced tree
775   mortality portends increased regional die-off under global-change-type drought.
776   *Proceedings of the National Academy of Sciences, 106*(17), 7063-7066.

777 Alduchov, O. A., & Eskridge, R. E. (1996). Improved Magnus form approximation of
778   saturation vapor pressure. *Journal of Applied Meteorology and Climatology, 35*(4),
779   601-609.
780 Allen, C. D. (2009). Climate-induced forest dieback: an escalating global phenomenon.
781   *Unasylva, 231*(232), 60.
782 Andreadis, K. M., Storck, P., & Lettenmaier, D. P. (2009). Modeling snow accumulation and
783   ablation processes in forested environments. *Water Resources Research, 45*(5).
784 Bartlett, P. A., MacKay, M. D., & Verseghy, D. L. (2006). Modified snow algorithms in the
785   Canadian land surface scheme: Model runs and sensitivity analysis at three boreal
786   forest stands. *Atmosphere-Ocean, 44*(3), 207-222. doi:10.3137/ao.440301
787 Bartlett, P. A., & Verseghy, D. L. (2015). Modified treatment of intercepted snow improves
788   the simulated forest albedo in the Canadian Land Surface Scheme. *Hydrological
789   Processes, 29*(14), 3208-3226. doi:10.1002/hyp.10431
790 Best, M. J. (2011). The Joint UK Land Environment Simulator (JULES), model description—
791   Part 1: Energy and water fluxes. *Geosci. Model Dev., 4*, 677-699.
792 Bormann, K. J., Brown, R. D., Derksen, C., & Painter, T. H. (2018). Estimating snow-cover
793   trends from space. *Nature Climate Change, 8*(11), 924-928. doi:10.1038/s41558-
794   018-0318-3
795 Broxton, P. D., van Leeuwen, W. J. D., & Biederman, J. A. (2019). Improving Snow Water
796   Equivalent Maps With Machine Learning of Snow Survey and Lidar Measurements.
797   *Water Resources Research, 55*(5), 3739-3757.
798   doi:https://doi.org/10.1029/2018WR024146
799 Bunnell, F. L., McNay, R. S., & Shank, C. C. (1985). *Trees and snow: the deposition of snow on
800   the ground: a review and quantitative synthesis*: Province of British Columbia.
801 Carlyle-Moses, D. E., & Gash, J. H. (2011). Rainfall interception loss by forest canopies. In
802   *Forest hydrology and biogeochemistry* (pp. 407-423): Springer.
803 Clark, M. P., Nijssen, B., Lundquist, J. D., Kavetski, D., Rupp, D. E., Woods, R. A., . . . Gochis, D. J.
804   (2015). A unified approach for process‐based hydrologic modeling: 2. Model
805   implementation and case studies. *Water Resources Research, 51*(4), 2515-2542.
806 Cristea, N. C., Lundquist, J. D., Loheide II, S. P., Lowry, C. S., & Moore, C. E. (2014). Modelling
807   how vegetation cover affects climate change impacts on streamflow timing and
808   magnitude in the snowmelt-dominated upper Tuolumne Basin, Sierra Nevada.
809   *Hydrological Processes, 28*(12), 3896-3918. doi:https://doi.org/10.1002/hyp.9909
810 Deems, J. S., Painter, T. H., & Finnegan, D. C. (2013). Lidar measurement of snow depth: a
811   review. *Journal of Glaciology, 59*(215), 467-479. doi:10.3189/2013JoG12J154
812 Dickerson-Lange, S. E., Gersonde, R. F., Hubbart, J. A., Link, T. E., Nolin, A. W., Perry, G. H., . . .
813   Lundquist, J. D. (2017). Snow disappearance timing is dominated by forest effects on
814   snow accumulation in warm winter climates of the Pacific Northwest, United States.
815   *Hydrological Processes, 31*(10), 1846-1862.
816 Ellis, C., Pomeroy, J., Brown, T., & MacDonald, J. (2010). Simulation of snow accumulation
817   and melt in needleleaf forest environments. *Hydrology and Earth System Sciences,
818   14*(6), 925-940.
819 Essery, R. (2015). A factorial snowpack model (FSM 1.0). *Geosci. Model Dev., 8*(12), 3867-
820   3876. doi:10.5194/gmd-8-3867-2015

821   Essery, R., Pomeroy, J., Parviainen, J., & Storck, P. (2003). Sublimation of Snow from
822   Coniferous Forests in a Climate Model. *Journal of Climate, 16*(11), 1855-1864.
823   doi:10.1175/1520-0442(2003)016<1855:Sosfcf>2.0.Co;2
824   Farnes, P. (1967). *Criteria for determining mountain snow pillow sites.* Paper presented at
825   the Proc. 35th western snow conf.
826   Feld, S. I., Cristea, N. C., & Lundquist, J. D. (2013). Representing atmospheric moisture
827   content along mountain slopes: Examination using distributed sensors in the Sierra
828   Nevada, California. *Water Resources Research, 49*(7), 4424-4441.
829   doi:https://doi.org/10.1002/wrcr.20318
830   Filhol, S., & Sturm, M. (2019). The smoothing of landscapes during snowfall with no wind.
831   *Journal of Glaciology, 65*(250), 173-187. doi:10.1017/jog.2018.104
832   Friesen, J., Lundquist, J., & Van Stan, J. T. (2015). Evolution of forest precipitation water
833   storage measurement methods. *Hydrological Processes, 29*(11), 2504-2520.
834   Gelfan, A., Pomeroy, J., & Kuchment, L. (2004). Modeling forest cover influences on snow
835   accumulation, sublimation, and melt. *Journal of Hydrometeorology, 5*(5), 785-803.
836   Goodell, B. (1959). *Management of forest stands in western United States to influence the
837   flow of snow-fed streams*: Association internationnale d'hydrologie scientifique.
838   Halofsky, J. E., Peterson, D. L., & Harvey, B. J. (2020). Changing wildfire, changing forests:
839   the effects of climate change on fire regimes and vegetation in the Pacific Northwest,
840   USA. *Fire Ecology, 16*(1), 4. doi:10.1186/s42408-019-0062-8
841   Hedstrom, N., & Pomeroy, J. (1998). Measurements and modelling of snow interception in
842   the boreal forest. *Hydrological Processes, 12*(10‐11), 1611-1625.
843   Helbig, N., Moeser, D., Teich, M., Vincent, L., Lejeune, Y., Sicart, J. E., & Monnet, J. M. (2020).
844   Snow processes in mountain forests: interception modeling for coarse-scale
845   applications. *Hydrol. Earth Syst. Sci., 24*(5), 2545-2560. doi:10.5194/hess-24-2545-
846   2020
847   Hoover, M. D., & Charles, F. (1967). *Leaf, 1967.* Paper presented at the Process and
848   significance of interception in Colorado subalpine forests. In Internatl. Symp. Forest
849   Hydrol. Oxyford and New York.
850   Huerta, M. L., Molotch, N. P., & McPhee, J. (2019). Snowfall interception in a deciduous
851   Nothofagus forest and implications for spatial snowpack distribution. *Hydrological
852   Processes, 33*(13), 1818-1834. doi:https://doi.org/10.1002/hyp.13439
853   Kim, E., Gatebe, C., Hall, D., Newlin, J., Misakonis, A., Elder, K., . . . De Marco, E. (2017). *NASA's
854   SnowEx campaign: Observing seasonal snow in a forested environment.* Paper
855   presented at the 2017 IEEE International Geoscience and Remote Sensing
856   Symposium (IGARSS).
857   Kim, R. S., Kumar, S., Vuyovich, C., Houser, P., Lundquist, J., Mudryk, L., . . . Wang, S. (2020).
858   Snow Ensemble Uncertainty Project (SEUP): Quantification of snow water
859   equivalent uncertainty across North America via ensemble land surface modeling.
860   *The Cryosphere Discuss., 2020*, 1-32. doi:10.5194/tc-2020-248
861   Kittredge, J. (1953). Influences of forests on snow in the ponderosa-sugar pine-fir zone of
862   the Central Sierra Nevada. *Hilgardia, 22*(1), 1-96.
863   Kobayashi, D. (1987). Snow accumulation on a narrow board. *Cold Regions Science and
864   Technology, 13*(3), 239-245.

865 Kozii, N., Laudon, H., Ottosson-Löfvenius, M., & Hasselquist, N. J. (2017). Increasing water
866   losses from snow captured in the canopy of boreal forests: A case study using a
867   30 year data set. *Hydrological Processes, 31*(20), 3558-3567.
868   doi:https://doi.org/10.1002/hyp.11277
869 Kuroiwa, D. (1967). Micromeritical properties of snow. *Physics of Snow and Ice, Hokkaido*
870   *Univ.*(2), 751-772.
871 Landry, C. C., Buck, K. A., Raleigh, M. S., & Clark, M. P. (2014). Mountain system monitoring
872   at Senator Beck Basin, San Juan Mountains, Colorado: A new integrative data source
873   to develop and evaluate models of snow and hydrologic processes. *Water Resources*
874   *Research, 50*(2), 1773-1788. doi:https://doi.org/10.1002/2013WR013711
875 Lapo, K., Nijssen, B., & Lundquist, J. D. (2019). Evaluation of Turbulence Stability Schemes
876   of Land Models for Stable Conditions. *Journal of Geophysical Research: Atmospheres,*
877   *124*(6), 3072-3089. doi:https://doi.org/10.1029/2018JD028970
878 Lawrence, D. M., Fisher, R. A., Koven, C. D., Oleson, K. W., Swenson, S. C., Bonan, G., . . . Zeng,
879   X. (2019). The Community Land Model Version 5: Description of New Features,
880   Benchmarking, and Impact of Forcing Uncertainty. *Journal of Advances in Modeling*
881   *Earth Systems, 11*(12), 4245-4287. doi:10.1029/2018ms001583
882 LeMone, M. A., Angevine, W. M., Bretherton, C. S., Chen, F., Dudhia, J., Fedorovich, E., . . . Weil,
883   J. (2019). 100 Years of Progress in Boundary Layer Meteorology. *Meteorological*
884   *Monographs, 59*, 9.1-9.85. doi:10.1175/amsmonographs-d-18-0013.1
885 Libbrecht, K. G. (2019). Snow crystals. *arXiv preprint arXiv:1910.06389*.
886 Liston, G. E., & Elder, K. (2006). A distributed snow-evolution modeling system
887   (SnowModel). *Journal of Hydrometeorology, 7*(6), 1259-1276.
888 Lundberg, A., & Halldin, S. (2001). Snow interception evaporation. Review of
889   measurementtechniques, processes, and models. *Theoretical and Applied*
890   *Climatology, 70*(1-4), 117-133.
891 Lundberg, A., Nakai, Y., Thunehed, H., & Halldin, S. (2004). Snow accumulation in forests
892   from ground and remote-sensing data. *Hydrological Processes, 18*(10), 1941-1955.
893   doi:https://doi.org/10.1002/hyp.1459
894 Lundquist, J. D., Dickerson-Lange, S. E., Lutz, J. A., & Cristea, N. C. (2013). Lower forest
895   density enhances snow retention in regions with warmer winters: A global
896   framework developed from plot‐scale observations and modeling. *Water Resources*
897   *Research, 49*(10), 6356-6370.
898 Lundquist, J. D., Neiman, P. J., Martner, B., White, A. B., Gottas, D. J., & Ralph, F. M. (2008).
899   Rain versus Snow in the Sierra Nevada, California: Comparing Doppler Profiling
900   Radar and Surface Observations of Melting Level. *Journal of Hydrometeorology, 9*(2),
901   194-211. doi:10.1175/2007jhm853.1
902 Mahat, V., & Tarboton, D. G. (2014). Representation of canopy snow interception, unloading
903   and melt in a parsimonious snowmelt model. *Hydrological Processes, 28*(26), 6320-
904   6336. doi:10.1002/hyp.10116
905 Martin, K. A., Van Stan II, J. T., Dickerson-Lange, S. E., Lutz, J. A., Berman, J. W., Gersonde, R.,
906   & Lundquist, J. D. (2013). Development and testing of a snow interceptometer to
907   quantify canopy water storage and interception processes in the rain/snow
908   transition zone of the North Cascades, Washington, USA. *Water Resources Research,*
909   *49*(6), 3243-3256. doi:https://doi.org/10.1002/wrcr.20271

910   Mazzotti, G., Currier, W. R., Deems, J. S., Pflug, J. M., Lundquist, J. D., & Jonas, T. (2019).
911   Revisiting Snow Cover Variability and Canopy Structure Within Forest Stands:
912   Insights From Airborne Lidar Data. *Water Resources Research, 55*(7), 6198-6216.
913   doi:https://doi.org/10.1029/2019WR024898
914   Mazzotti, G., Essery, R., Moeser, C. D., & Jonas, T. (2020). Resolving Small-Scale Forest Snow
915   Patterns Using an Energy Balance Snow Model With a One-Layer Canopy. *Water*
916   *Resources Research, 56*(1), e2019WR026129.
917   doi:https://doi.org/10.1029/2019WR026129
918   Mazzotti, G., Essery, R., Webster, C., Malle, J., & Jonas, T. (2020). Process-Level Evaluation of
919   a Hyper-Resolution Forest Snow Model Using Distributed Multisensor Observations.
920   *Water Resources Research, 56*(9), e2020WR027572.
921   doi:https://doi.org/10.1029/2020WR027572
922   Merriam, R. A. (1960). A note on the interception loss equation. *Journal of Geophysical*
923   *Research, 65*(11), 3850-3851.
924   Miller, D. H. (1962). Snow in the Trees: Where Does it Go? *Proceedings of the Western Snow*
925   *Conference, 30*, 21-27.
926   Miller, D. H. (1966). *Transport of intercepted snow from trees during snow storms*. Pacific
927   Southwest Forest and Range Experiment Station, Forest Service, USA.
928   Moeser, D., Mazzotti, G., Helbig, N., & Jonas, T. (2016). Representing spatial variability of
929   forest snow: Implementation of a new interception model. *Water Resources*
930   *Research, 52*(2), 1208-1226. doi:10.1002/2015wr017961
931   Moeser, D., Stähli, M., & Jonas, T. (2015). Improved snow interception modeling using
932   canopy parameters derived from airborne LiDAR data. *Water Resources Research,*
933   *51*(7), 5041-5059. doi:10.1002/2014wr016724
934   Murray, F. W. (1966). *On the computation of saturation vapor pressure*. Retrieved from
935   Nakaya, U. (1954). Snow crystals: natural and artificial.
936   Niu, G.-Y., Yang, Z.-L., Mitchell, K. E., Chen, F., Ek, M. B., Barlage, M., . . . Xia, Y. (2011). The
937   community Noah land surface model with multiparameterization options (Noah-
938   MP): 1. Model description and evaluation with local-scale measurements. *Journal of*
939   *Geophysical Research: Atmospheres, 116*(D12). doi:10.1029/2010jd015139
940   Niu, G.-Y., & Yang, Z. L. (2004). Effects of vegetation canopy processes on snow surface
941   energy and mass balances. *Journal of Geophysical Research: Atmospheres, 109*(D23).
942   Perket, J. (2015). *Diagnosis and Improvement of Cryosphere Shortwave Radiation Biases in*
943   *Global Climate Models.* (Ph.D.), University of Michigan, Retrieved from
944   http://hdl.handle.net/2027.42/113453
945   Pfister, R., & Schneebeli, M. (1999). Snow accumulation on boards of different sizes and
946   shapes. *Hydrological Processes, 13*(14‐15), 2345-2355.
947   Pflug, J. M., Liston, G. E., Nijssen, B., & Lundquist, J. D. (2019). Testing Model
948   Representations of Snowpack Liquid Water Percolation Across Multiple Climates.
949   *Water Resources Research, 55*(6), 4820-4838.
950   doi:https://doi.org/10.1029/2018WR024632
951   Pomeroy, J. W., Gray, D. M., Brown, T., Hedstrom, N. R., Quinton, W. L., Granger, R. J., & Carey,
952   S. K. (2007). The cold regions hydrological model: a platform for basing process
953   representation and model structure on physical evidence. *Hydrological Processes,*
954   *21*(19), 2650-2667. doi:https://doi.org/10.1002/hyp.6787

Pomeroy, J. W., & Schmidt, R. A. (1993). *The use of fractal geometry in modelling intercepted snow accumulation and sublimation.* Paper presented at the Proceedings of the Eastern Snow Conference.

Qu, X., & Hall, A. (2014). On the persistent spread in snow-albedo feedback. *Climate Dynamics, 42*(1), 69-81. doi:10.1007/s00382-013-1774-0

Raleigh, M. S., & Lundquist, J. D. (2012). Comparing and combining SWE estimates from the SNOW-17 model using PRISM and SWE reconstruction. *Water Resources Research, 48*(1). doi:10.1029/2011wr010542

Revuelto, J., López-Moreno, J. I., Azorin-Molina, C., & Vicente-Serrano, S. M. (2015). Canopy influence on snow depth distribution in a pine stand determined from terrestrial laser data. *Water Resources Research, 51*(5), 3476-3489. doi:https://doi.org/10.1002/2014WR016496

Rittger, K., Raleigh, M. S., Dozier, J., Hill, A. F., Lutz, J. A., & Painter, T. H. (2020). Canopy Adjustment and Improved Cloud Detection for Remotely Sensed Snow Cover Mapping. *Water Resources Research, 56*(6), e2019WR024914. doi:https://doi.org/10.1029/2019WR024914

Roesch, A., Wild, M., Gilgen, H., & Ohmura, A. (2001). A new snow cover fraction parametrization for the ECHAM4 GCM. *Climate Dynamics, 17*(12), 933-946.

Roth, T. R., & Nolin, A. W. Characterizing Maritime Snow Canopy Interception in Forested Mountains. *Water Resources Research, 55*(0), 15. doi:10.1029/2018wr024089

Rutter, N., Essery, R., Pomeroy, J., Altimir, N., Andreadis, K., Baker, I., . . . Deng, H. (2009). Evaluation of forest snow processes models (SnowMIP2). *Journal of Geophysical Research: Atmospheres, 114*(D6). doi:10.1029/2008JD011063

Satterlund, D. R., & Haupt, H. F. (1967). Snow catch by Contier Crowns. *Water Resources Research, 3*(4), 1035-1039. doi:10.1029/WR003i004p01035

Satterlund, D. R., & Haupt, H. F. (1970). The Disposition of Snow Caught by Conifer Crowns. *Water Resources Research, 6*(2), 649-652. doi:10.1029/WR006i002p00649

Sazaki, G., Zepeda, S., Nakatsubo, S., Yokomine, M., & Furukawa, Y. (2012). Quasi-liquid layers on ice crystal surfaces are made up of two different phases. *Proceedings of the National Academy of Sciences, 109*(4), 1052. doi:10.1073/pnas.1116685109

Schmidt, R. A. (1972). *Sublimation of wind-transported snow: a model* (Vol. 90): Rocky Mountain Forest and Range Experiment Station, Forest Service, US ....

Schmidt, R. A. (1991). Sublimation of snow intercepted by an artificial conifer. *Agricultural and Forest Meteorology, 54*(1), 1-27.

Schmidt, R. A., & Gluns, D. R. (1991). Snowfall interception on branches of three conifer species. *Canadian Journal of Forest Research, 21*(8), 1262-1269.

Sexstone, G. A., Clow, D. W., Fassnacht, S. R., Liston, G. E., Hiemstra, C. A., Knowles, J. F., & Penn, C. A. (2018). Snow Sublimation in Mountain Environments and Its Sensitivity to Forest Disturbance and Climate Warming. *Water Resources Research, 54*(2), 1191-1211. doi:https://doi.org/10.1002/2017WR021172

Shampine, L. F., & Reichelt, M. W. (1997). The matlab ode suite. *SIAM journal on scientific computing, 18*(1), 1-22.

Shidei, T. (1952). Study of the fallen snow on the forest trees. I. *Bull. Gov. For. Exp. Stn., 54*, 115-164.

999   Stewart, R. E., Thériault, J. M., & Henson, W. (2015). On the Characteristics of and Processes
1000   Producing Winter Precipitation Types near 0°C. *Bulletin of the American*
1001   *Meteorological Society, 96*(4), 623-639. doi:10.1175/bams-d-14-00032.1
1002   Storck, P. (2000). Trees, snow and flooding: An investigation of forest canopy effects on
1003   snow accumulation and melt at the plot and watershed scales in the Pacific
1004   Northwest.
1005   Storck, P., Lettenmaier, D. P., & Bolton, S. M. (2002). Measurement of snow interception and
1006   canopy effects on snow accumulation and melt in a mountainous maritime climate,
1007   Oregon, United States. *Water Resources Research, 38*(11), 5-1-5-16.
1008   Strasser, U., Bernhardt, M., Weber, M., Liston, G. E., & Mauser, W. (2007). Is snow
1009   sublimation important in the alpine water balance? *The Cryosphere Discussions, 1*(2),
1010   303-350.
1011   Strasser, U., Warscher, M., & Liston, G. E. (2011). Modeling Snow–Canopy Processes on an
1012   Idealized Mountain. *Journal of Hydrometeorology, 12*(4), 663-677.
1013   doi:10.1175/2011jhm1344.1
1014   Sun, N., Wigmosta, M., Zhou, T., Lundquist, J., Dickerson-Lange, S., & Cristea, N. (2018).
1015   Evaluating the functionality and streamflow impacts of explicitly modelling forest–
1016   snow interactions and canopy gaps in a distributed hydrologic model. *Hydrological*
1017   *Processes, 32*(13), 2128-2140. doi:10.1002/hyp.13150
1018   Teich, M., Giunta, A. D., Hagenmuller, P., Bebi, P., Schneebeli, M., & Jenkins, M. J. (2019).
1019   Effects of bark beetle attacks on forest snowpack and avalanche formation –
1020   Implications for protection forest management. *Forest Ecology and Management,*
1021   *438*, 186-203. doi:https://doi.org/10.1016/j.foreco.2019.01.052
1022   Thackeray, C. W., & Fletcher, C. G. (2016). Snow albedo feedback:Current knowledge,
1023   importance, outstanding issues and future directions. *Progress in Physical*
1024   *Geography: Earth and Environment, 40*(3), 392-408.
1025   doi:10.1177/0309133315620999
1026   Thackeray, C. W., Fletcher, C. G., & Derksen, C. (2014). The influence of canopy snow
1027   parameterizations on snow albedo feedback in boreal forest regions. *Journal of*
1028   *Geophysical Research: Atmospheres, 119*(16), 9810-9821.
1029   Thorpe, A., & Mason, B. (1966). The evaporation of ice spheres and ice crystals. *British*
1030   *Journal of Applied Physics, 17*(4), 541.
1031   USACE. (1956). Snow hydrology: Summary Rep. of the Snow Investigations. *, North Pacific*
1032   *Division, Portland, OR*.
1033   Vuyovich, C. M., Jacobs, J. M., & Daly, S. F. (2014). Comparison of passive microwave and
1034   modeled estimates of total watershed SWE in the continental United States. *Water*
1035   *Resources Research, 50*(11), 9088-9102.
1036   doi:https://doi.org/10.1002/2013WR014734
1037   Watanabe, S., & Ozeki, J. (1964). Study of fallen snow on forest trees (II). Experiment on the
1038   snow crown of the Japanese cedar. *Jap. Govt. Forest Exp. Sta. Bull, 169*, 121-140.
1039   Wayand, N. E., Clark, M. P., & Lundquist, J. D. (2017). Diagnosing snow accumulation errors
1040   in a rain-snow transitional environment with snow board observations.
1041   *Hydrological Processes, 31*(2), 349-363. doi:10.1002/hyp.11002
1042   Wayand, N. E., Stimberis, J., Zagrodnik, J. P., Mass, C. F., & Lundquist, J. D. (2016). Improving
1043   simulations of precipitation phase and snowpack at a site subject to cold air

1044   intrusions: Snoqualmie Pass, WA. *Journal of Geophysical Research: Atmospheres,*
1045   *121*(17), 9929-9942.
1046 Webster, C., & Jonas, T. (2018). Influence of canopy shading and snow coverage on effective
1047   albedo in a snow-dominated evergreen needleleaf forest. *Remote sensing of*
1048   *environment, 214*, 48-58. doi:https://doi.org/10.1016/j.rse.2018.05.023
1049 White, J. C., Coops, N. C., Wulder, M. A., Vastaranta, M., Hilker, T., & Tompalski, P. (2016).
1050   Remote Sensing Technologies for Enhancing Forest Inventories: A Review. *Canadian*
1051   *Journal of Remote Sensing, 42*(5), 619-641. doi:10.1080/07038992.2016.1207484
1052

1054 **Table 1**: *Canopy interception representations in commonly-used hydrologic land surface models, as well as a selection of snow*

1055 *models*

1056 Note: For each process, ✓=yes, included, and blank indicates not included. Model citations are as follows: CRHM (Ellis, Pomeroy,

1057 Brown, & MacDonald, 2010; Pomeroy et al., 2007); VISA (Niu and Yang 2004); CLASS (Bartlett et al. 2006; Bartlett and Verseghy

1058 2015); UEB (Mahat & Tarboton, 2014); VIC & DHSVM (Andreadis et al. 2009); SUMMA (Clark et al. 2015ab); Noah-MP (Niu et

1059 al., 2011); JULES (Best, 2011; Essery, Pomeroy, Parviainen, & Storck, 2003); CLM (Lawrence et al., 2019); SnowModel (Liston &

1060 Elder, 2006) ; FSM (Essery, 2015; Mazzotti, Essery, Moeser, et al., 2020; Moeser, Mazzotti, Helbig, & Jonas, 2016; Moeser et al.,

1061 2015) ; AMUNDSEN (Strasser, Bernhardt, Weber, Liston, & Mauser, 2007; Strasser, Warscher, & Liston, 2011);

	CRHM	VISA	CLASS	UEB	VIC/ DHSVM	SUMMA	Noah-MP	JULES	CLM	Snow Model	FSM	AMUNDSEN
Tracks canopy snow temperature					✓							
Models melt of intercepted snow		✓		✓	✓	✓	✓	✓				✓
Interception efficiency asymptotes to 0 as I → I_{max} (exponential function)	✓	✓	✓	✓	✓	✓	✓	✓	✓	✓	✓Mazzotti	✓

Interception efficiency asymptotes to 0 as I → I_{max} (sigmoidal function)											✓Moeser	
I_{max} function of density as defined by temperature	✓	✓	✓	✓		✓	✓					
I_{max} increases with temperature above -3°C					✓	✓						
Unloading exponential function of time	✓			✓		✓					✓Mazzotti	
Unloading at temperatures at or above 0°C:	✓	✓	✓		✓	✓	✓	✓	✓	✓	✓	✓
Full unloading	✓											
Partial unloading $f(T_{air})$ near or above 0°C		✓	✓		✓	✓	✓	✓	✓	✓	✓	✓
**unloaded as all solid	✓	✓	✓			✓*			✓	✓	✓	✓
** unloaded as mix (solid & liquid)					✓	✓		✓				
Unloading as a function of wind speed		✓	✓			✓*	✓		✓			

Sublimation modeled based on the rate of loss from an ice sphere	✓										✓		✓
Sublimation modeled as a function the wind profiles through the canopy, vapor pressure gradients, and aerodynamic resistance terms		✓	✓	✓	✓	✓	✓	✓	✓		✓Mazzotti	
Sublimation modeled as a function of incoming solar radiation											✓Moeser	

1062   ** VIC, DHSVM, and JULES unload snow at 40% of the canopy snowmelt rate; Others unload independently of melt rate (or without

1063   allowing melt to occur)

1064   *only in SUMMA 3.0 and later (https://github.com/NCAR/summa), not in the original; Note that SUMMA is a modular model

1065   framework and could be set up with or without these parameters.

1066 **Table 2. Study site meteorology for 1 December to 1 April**

1067 Note: Potential melt and sublimation were calculated using the baseline model parameters and

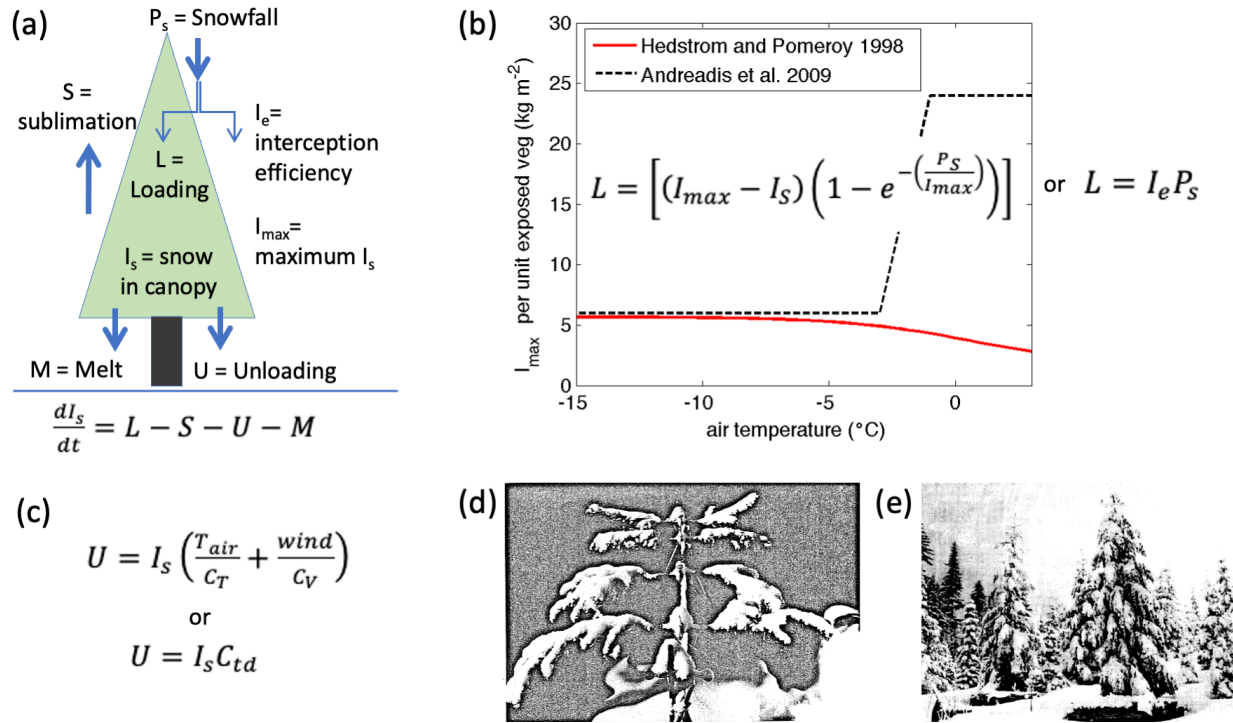1068 equations, assuming there was always canopy snow available to melt or sublimate.

Site	Analysis Water Year	Mean air temp-erature (°C)	Total precip-itation (mm)	Mean relative humidity (%)	Mean wind speed (m/s)	Potential melt (mm)	Potential sublimation (mm)
Umpqua, OR	1997-1998	0	639	92	1.5	392	116
Senator Beck, CO (Swamp Angel)	2008-2009	-7	533	65	1.2	205	961

1069

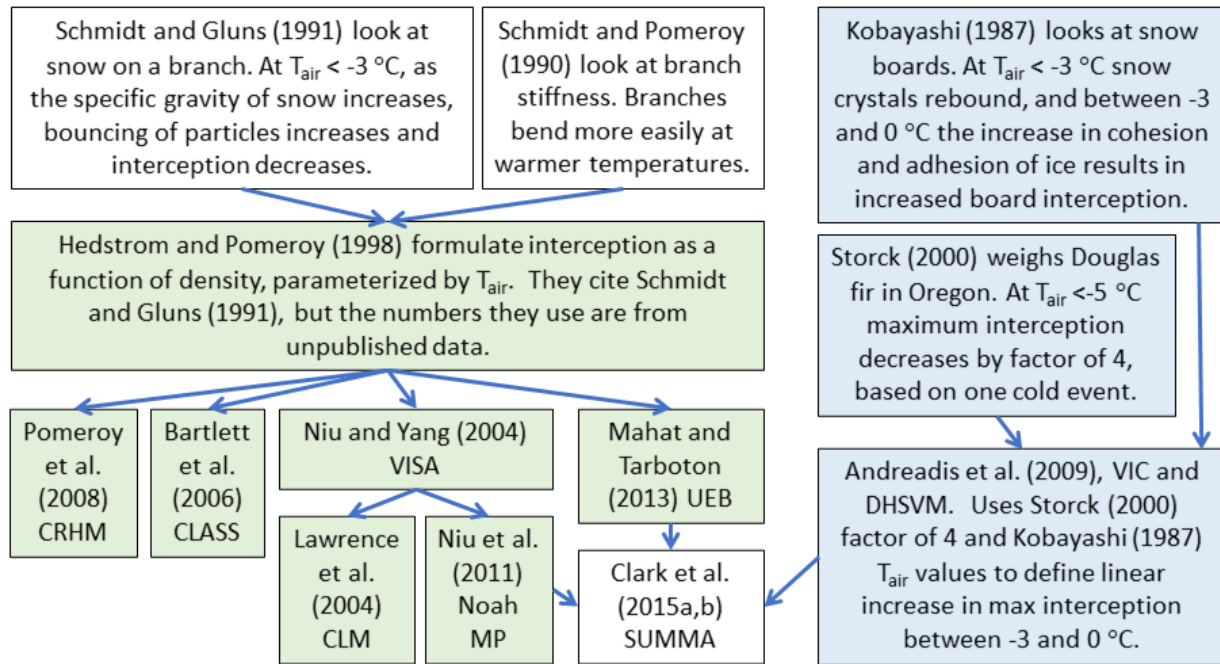1070 **Table 3. iModel Parameter Settings**

1071 *Rain falling at temperatures below the rain-snow cutoff (RScutoff) is assumed to be all snowfall,*

1072 *with all rainfall above. Sources for parameter values: (a) Storck et al. (2000); (b) Andreadis et*

1073 *al. (2009); (c) Martin et al. (2013), see their Table 1 for maximum measured intercepted snow in*

1074 *different climates; (d) Raleigh and Lundquist (2012) ; (e) Lundberg and Halldin (2001); (f)*

1075 *Lundquist et al. (2008); (g) Roesch et al. (2001); (h) Mahat and Tarboton (2014).*

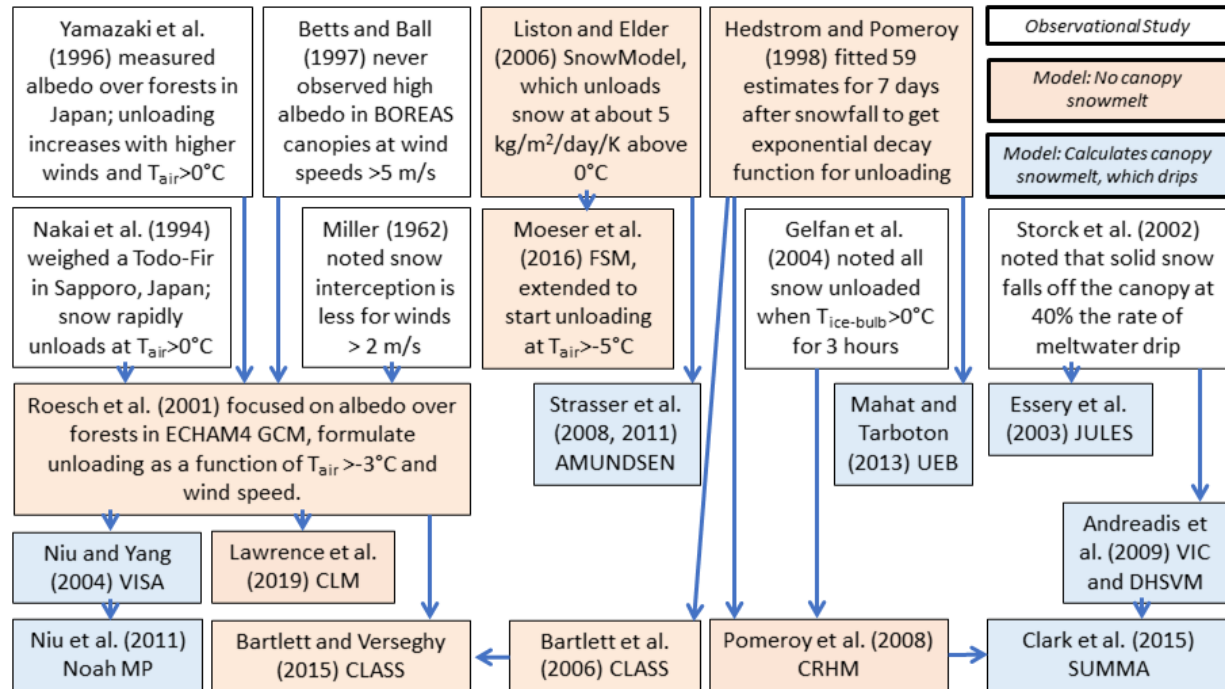| Name	Units	T-wind unloading	Exponential-decay unloading
M_T	-	0.25	0
M_v	-	0.25	0
M_{td}	-	0	1
$I_e min$	mm	0.6 [a]	
$I_e scale$	mm °C^{-1}	0.4 [b]	
$I_{max}min$	mm	20 [c]	
$I_{max}scale$	mm °C^{-1}	65 [c]	
M_{fac}	mm °C^{-1} hr^{-1}	4/24 [d]	
C_{sub}	mm Pa^{-1} m^{-1} s	0.002 [e]	
RScutoff	°C	1.5 [f]	
C_T	s^{-1}	1.87 x 10^5 [g]	
C_v	s^{-1}	1.56 x 10^5 [g]	
C_{td}	s^{-1}	1.2861 x 10^{-6} [h]	

1076

1077 **FIGURES**

1078

1079

1080 **Fig. 1.** *(a) Illustration of canopy processes and parameters in land surface models: trees*

1081 *intercept snow with a fractional efficiency (I_e) up to a maximum value (I_{max}), and the remaining*

1082 *snowfall passes through the canopy. Snow in the canopy (I_s) may sublimate, melt, or unload. (b)*

1083 *Loading may be parameterized as a function dependent on I_{max} or not, and loading capacity may*

1084 *or may not increase with temperature. (c) Unloading may be a function of air temperature (T_{air})*

1085 *and wind or may be a constant rate proportional to intercepted snow. (d) Branches clipped to a*

1086 *pole in the Rocky Mountains (Schmidt & Gluns, 1991).   (e) Douglas Firs in weighing*

1087 *lysimeters in the Oregon Cascades (Storck, 2000).*

Schmidt and Gluns (1991) look at snow on a branch. At T_{air} < -3 °C, as the specific gravity of snow increases, bouncing of particles increases and interception decreases.

Schmidt and Pomeroy (1990) look at branch stiffness. Branches bend more easily at warmer temperatures.

Kobayashi (1987) looks at snow boards. At T_{air} < -3 °C snow crystals rebound, and between -3 and 0 °C the increase in cohesion and adhesion of ice results in increased board interception.

Hedstrom and Pomeroy (1998) formulate interception as a function of density, parameterized by T_{air}. They cite Schmidt and Gluns (1991), but the numbers they use are from unpublished data.

Storck (2000) weighs Douglas fir in Oregon. At T_{air} <-5 °C maximum interception decreases by factor of 4, based on one cold event.

Pomeroy et al. (2008) CRHM

Bartlett et al. (2006) CLASS

Niu and Yang (2004) VISA

Mahat and Tarboton (2013) UEB

Lawrence et al. (2004) CLM

Niu et al. (2011) Noah MP

Clark et al. (2015a,b) SUMMA

Andreadis et al. (2009), VIC and DHSVM. Uses Storck (2000) factor of 4 and Kobayashi (1987) T_{air} values to define linear increase in max interception between -3 and 0 °C.

1088

1089 **Figure 2.** *Flow path of model development between the Hedstrom and Pomeroy vs. Andreadis*

1090 *I_{max} formulations shown in Fig. 1. Models listed in green boxes employ the solid red line in Fig.*

1091 *1b (and formulas 2 & 3), while models listed in the blue boxes employ the black dashed line in*

1092 *Fig. 1b to model maximum interception as a function of temperature.*
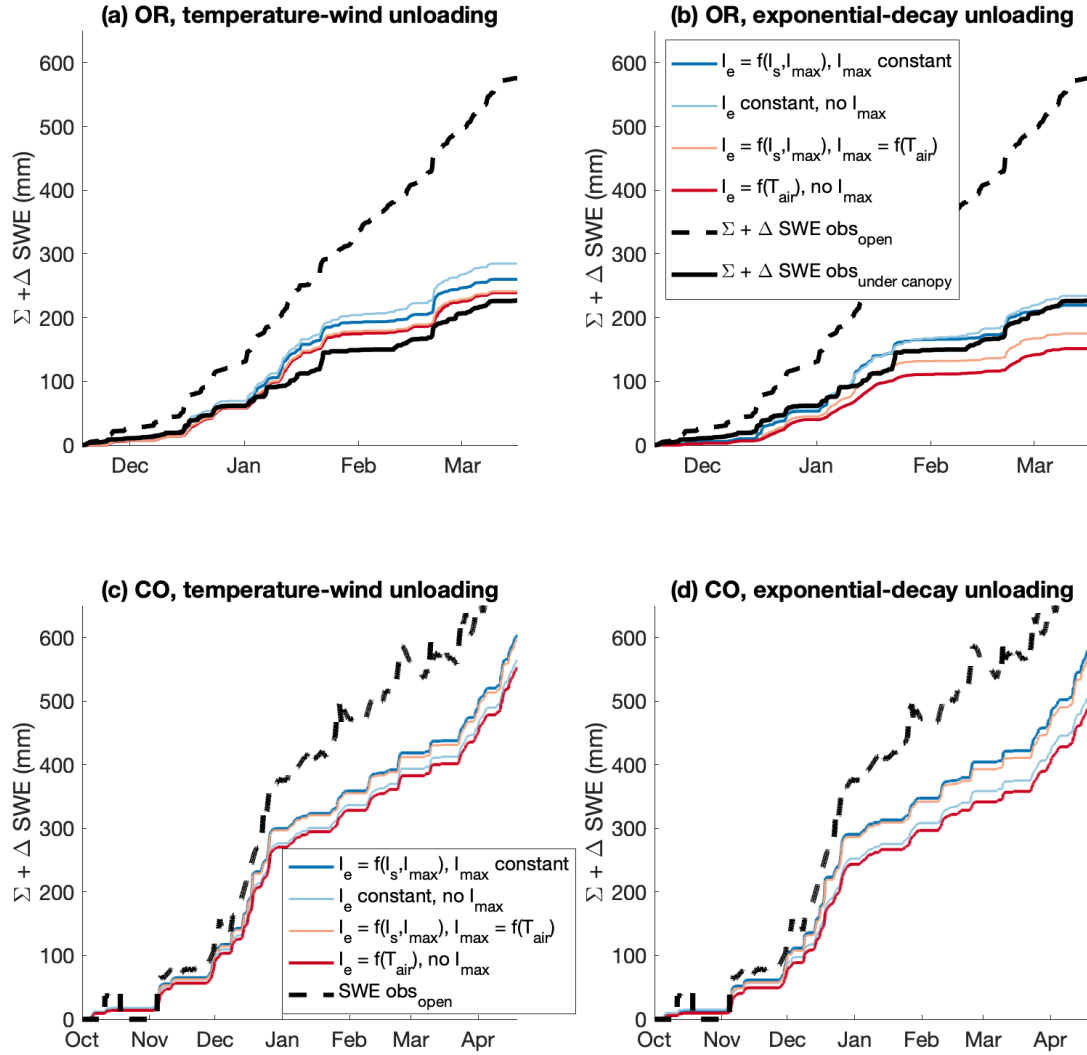
1093 .

1094

Figure 3. *History of model development for snow unloading. Arrows indicate flow of information through paper citations, while blue colors represent models that calculate snowmelt, which is then lost from the canopy through melt water drip, and orange colors indicate models that do not calculate canopy snowmelt. White boxes are observational studies and not models.*

.
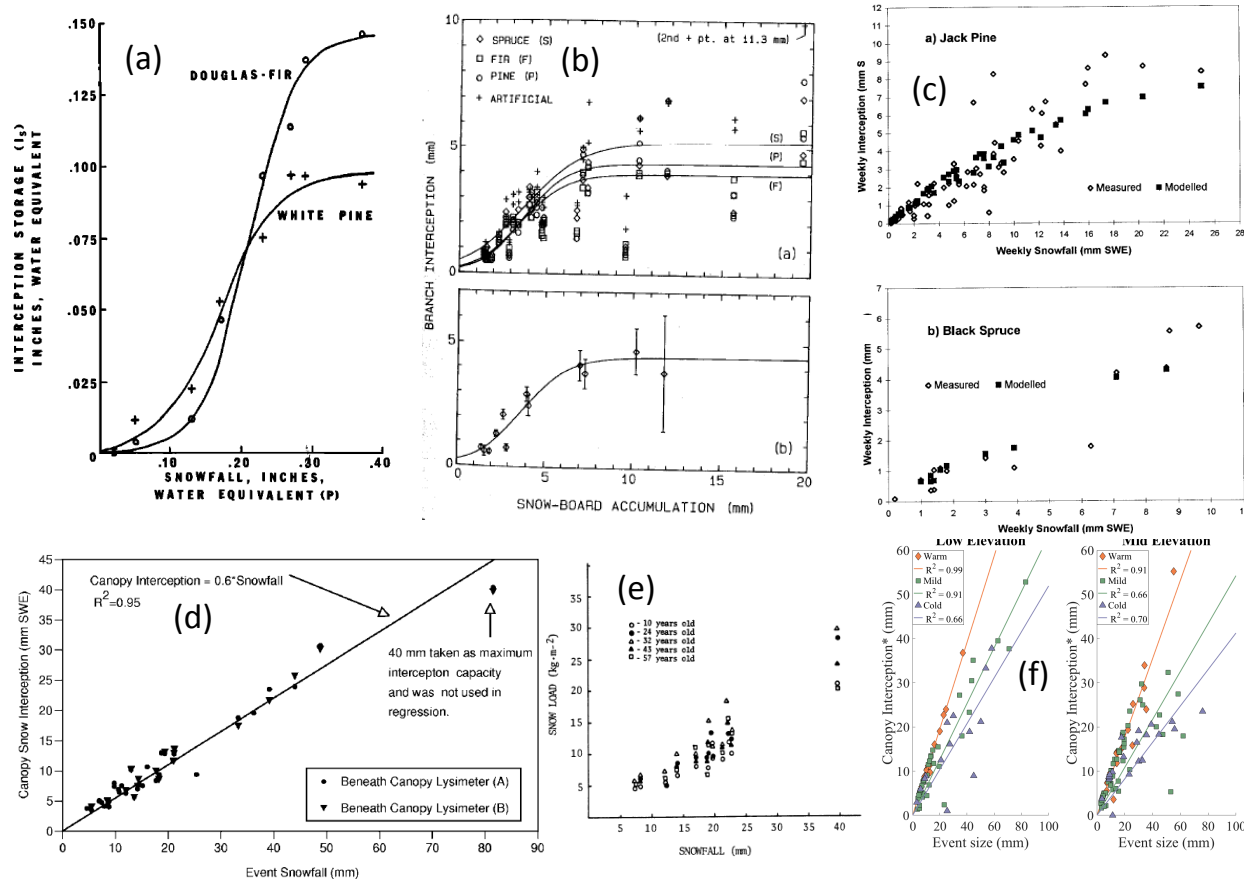
Figure 4. *(a) from Satturlund and Haupt (1967)'s Fig. 2, curves for two saplings for one storm event; (b) from Schmidt and Gluns (1991)'s Fig. 4, note large scatter of points around drawn curves as well as notation of a point off the top of the plotting range; (c) from Hedstrom and Pomeroy 1998's Fig. 6, note that modeled (filled squares) level off but that measured (diamonds) diverge from the model at high values; (d) from Storck 2000's Fig. 5.4, note single point taken as I_{max}, which does not diverge much from a linear fit; (e) from Watanabe and Ozeki 1964, as translated in Bunnell et al. 1985, their Fig 7.31; (f) from Roth and Nolin 2019's Fig. 5, note lack of any data suggesting a leveling off at I_{max}.*

(a) OR, temperature-wind unloading

(b) OR, exponential-decay unloading

- $I_e = f(I_s, I_{max})$, I_{max} constant
- I_e constant, no I_{max}
- $I_e = f(I_s, I_{max})$, $I_{max} = f(T_{air})$
- $I_e = f(T_{air})$, no I_{max}
- $\Sigma + \Delta$ SWE obs$_{open}$
- $\Sigma + \Delta$ SWE obs$_{under\ canopy}$

(c) CO, temperature-wind unloading

(d) CO, exponential-decay unloading

- $I_e = f(I_s, I_{max})$, I_{max} constant
- I_e constant, no I_{max}
- $I_e = f(I_s, I_{max})$, $I_{max} = f(T_{air})$
- $I_e = f(T_{air})$, no I_{max}
- SWE obs$_{open}$

Figure 5. *Timeseries of (a,b) modeled, with default parameters in Table 3, and observed snow accumulation on the ground under the canopy for Umpqua, Oregon (OR) for water year 1997-1998 and (c,d) for Swamp Angel, Senator Beck, Colorado (CO) for water year 2008-2009. Columns refer to unloading schemes, while colors refer to loading configurations. Warmer colors representing interception schemes with greater interception amounts at warmer temperatures. Snow accumulation ($\Sigma + \Delta SWE$) is represented by the cumulative sum of SWE increases, available for the Oregon site from a weighing lysimeter. Actual SWE is shown for the Colorado site, which, because little melt occurred during this period, matches well with modeled cumulative SWE in the open.*
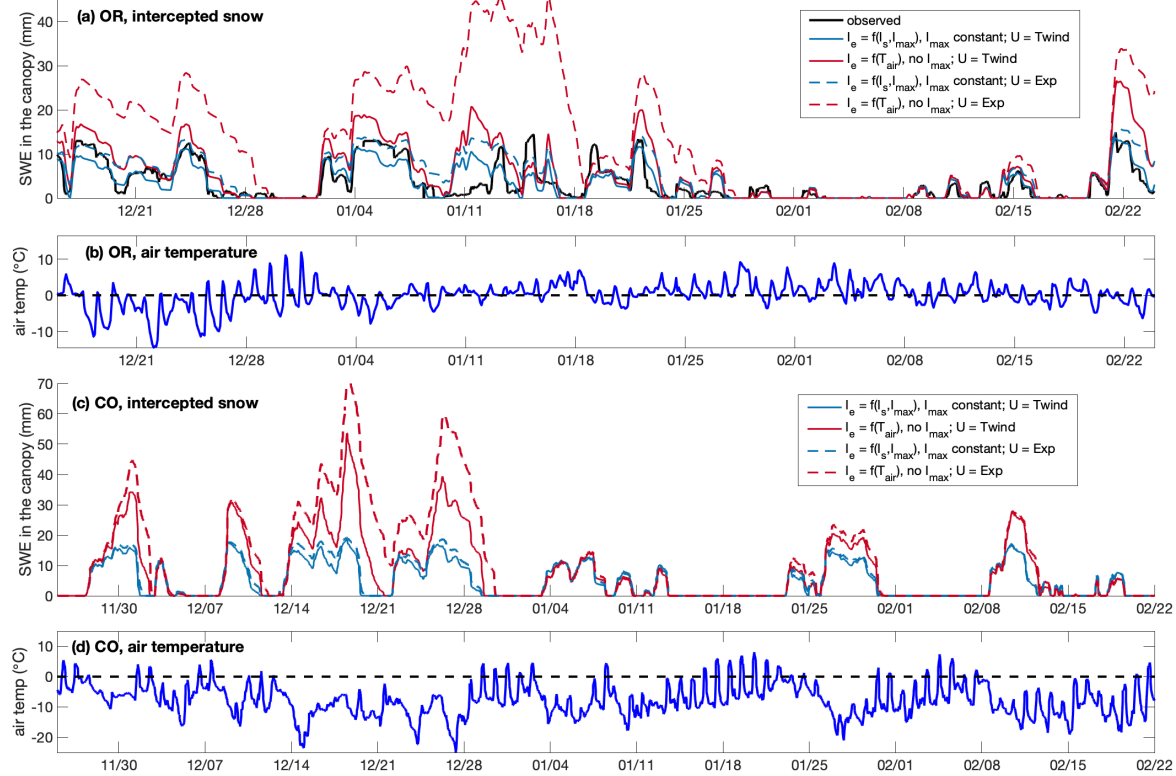
Figure 6. *Intercepted snow (a) and temperature (b) for 1997-1998 at Umpqua, Oregon and (c,d) for 2008-2009 at Senator Beck, Colorado (subset of time-periods shown in Fig. 5), where colored lines refer to the loading schemes as in Section 3, and line styles represent variations in canopy unloading. Model parameters are for baseline simulations in Table 2. Black lines (a) show intercepted snow from a Ponderosa Pine tree cut and weighed on a lysimeter.*
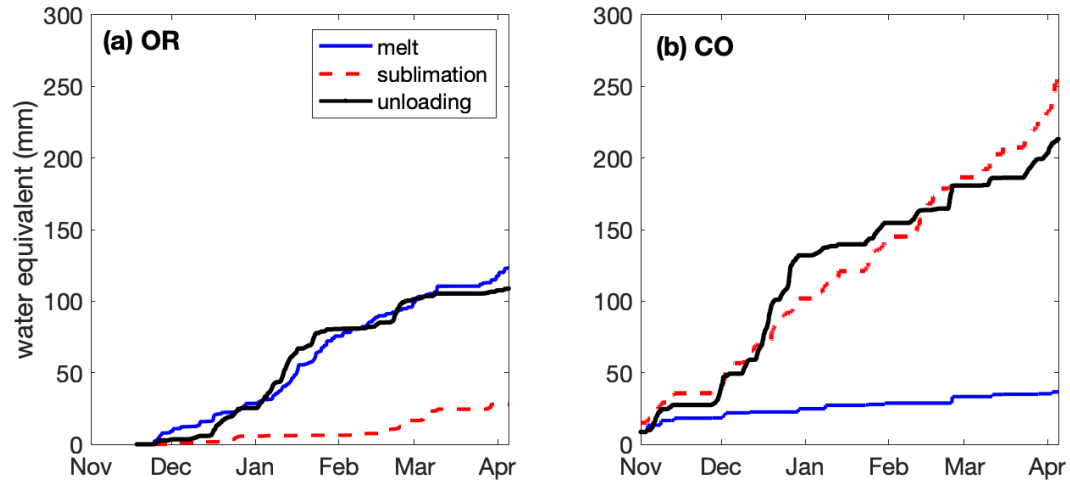
Figure 7. *Cumulative losses of snow water equivalent from the canopy for (a) Umpqua, Oregon and (b) Senator Beck Colorado, for the baseline simulation using the temperature-wind unloading parameterization and the loading scheme of $I_e=f(T_{air})$ and no I_{max}.*

1145

1146
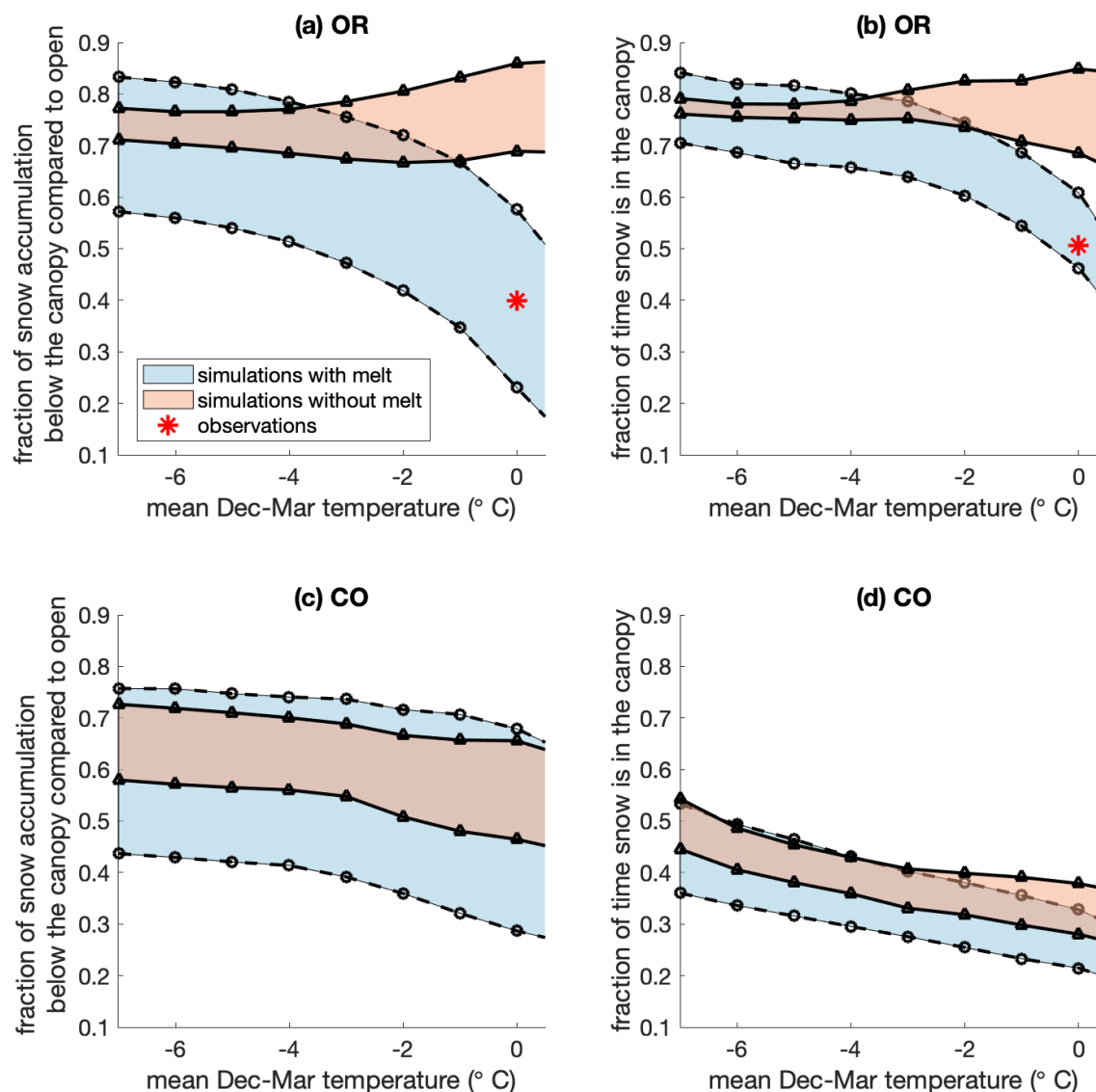
Figure 8. *Temperature change sensitivity for (a,b) Umpqua, OR for year 1997-98 and for (c,d)*

Senator Beck, CO for year 2008-09 for multiple model configurations with regards to (a,c) the

fraction of seasonal-total snow accumulating under the canopy compared to the open and (b,d)

the fraction of time when snow is present in the canopy. For reference, observed mean

temperature for Oregon was 0°C and for Colorado was -7°C, so in general, Oregon

temperatures were cooled while Colorado temperatures were warmed to compare results

assuming similar mean temperatures. The fractions observed at the Oregon site are plotted at

the observed mean temperature.

1155
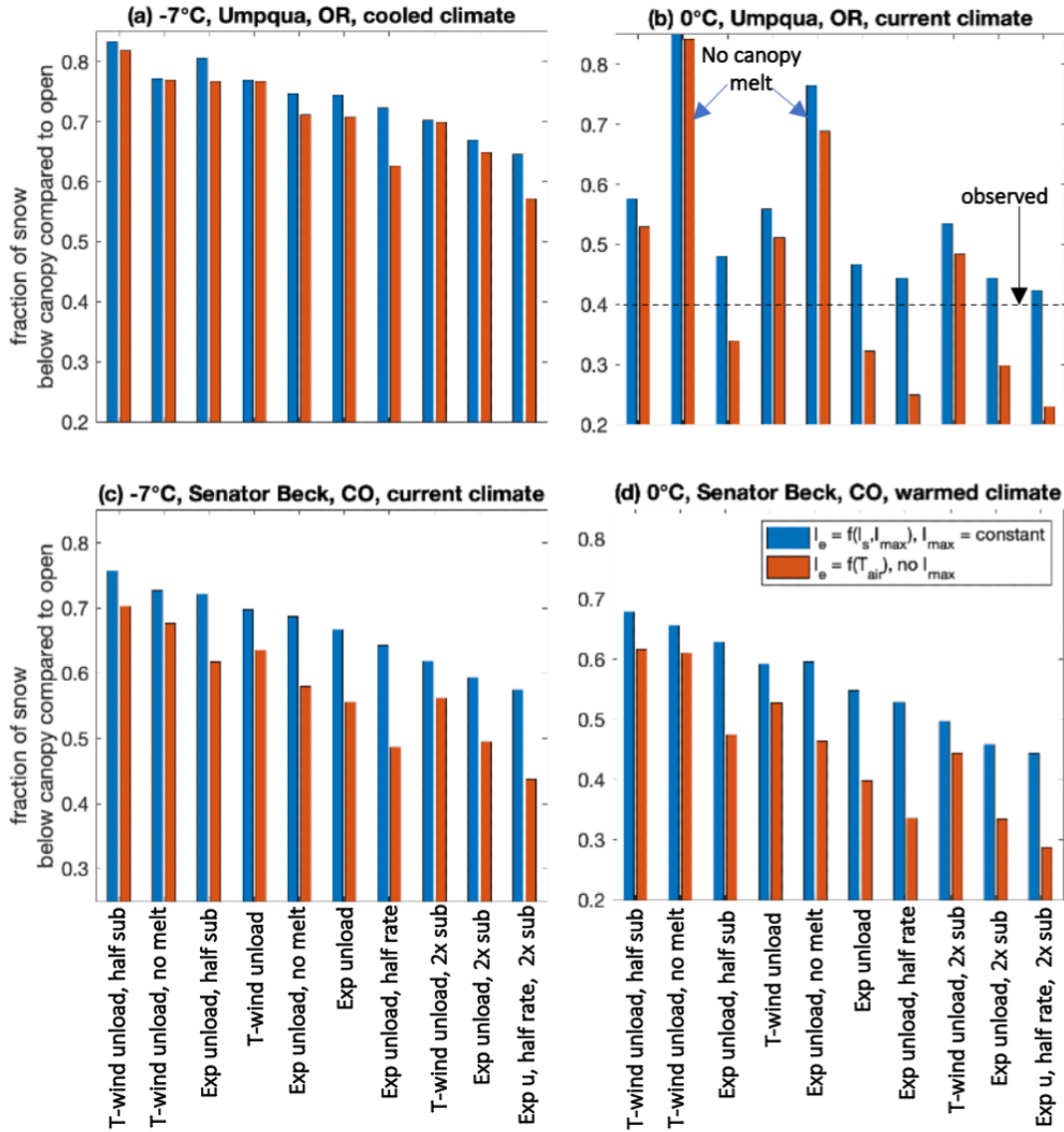
Figure 9. *Fraction of snow below the canopy compared to the open, as in Figure 8, but specifying specific run values at mean December to March temperatures of -7℃ (observed at the CO site) and at 0℃ (observed at the Oregon site). The value observed at the Oregon site is marked with a horizontal dashed line in (b).*

1164   **FIGURE LEGENDS**

1165

1166   **Figure 1.** (a) Illustration of canopy processes and parameters in land surface models: trees

1167   intercept snow with a fractional efficiency (I_e) up to a maximum value (I_{max}), and the remaining

1168   snowfall passes through the canopy. Snow in the canopy (I_s) may sublimate, melt, or unload. (b)

1169   Loading may be parameterized as a function dependent on I_{max} or not, and loading capacity may

1170   or may not increase with temperature. (c) Unloading may be a function of air temperature (T_{air})

1171   and wind or may be a constant rate proportional to intercepted snow. (d) Branches clipped to a

1172   pole in the Rocky Mountains (Schmidt & Gluns, 1991). (e) Douglas Firs in weighing lysimeters

1173   in the Oregon Cascades (Storck, 2000).

1174

1175   **Figure 2.** Flow path of model development between the Hedstrom and Pomeroy vs. Andreadis

1176 I_{max} formulations shown in Fig. 1. Models listed in green boxes employ the solid red line in Fig.

1177   1b (and formulas 2 & 3), while models listed in the blue boxes employ the black dashed line in

1178   Fig. 1b to model maximum interception as a function of temperature.

1179

1180   **Figure 3**. History of model development for snow unloading. Arrows indicate flow of

1181   information through paper citations, while blue colors represent models that calculate snowmelt,

1182   which is then lost from the canopy through melt water drip, and orange colors indicate models

1183   that do not calculate canopy snowmelt. White boxes are observational studies and not models.

1184

1185   **Figure 4**. (a) from Satturlund and Haupt (1967)'s Fig. 2, curves for two saplings for one storm

1186   event; (b) from Schmidt and Gluns (1991)'s Fig. 4, note large scatter of points around drawn

1187   curves as well as notation of a point off the top of the plotting range; (c) from Hedstrom and

1188   Pomeroy 1998's Fig. 6, note that modeled (filled squares) level off but that measured (diamonds)

1189   diverge from the model at high values; (d) from Storck 2000's Fig. 5.4, note single point taken as

1190 I_{max}, which does not diverge much from a linear fit; (e) from Watanabe and Ozeki (1964), as

1191   translated in Bunnell et al. 1985, their Fig 7.31; (f) from Roth and Nolin 2019's Fig. 5, note lack

1192   of any data suggesting a leveling off at I_{max}.

1193

1194 **Figure 5.** Timeseries of (a,b) modeled, with default parameters in Table 3, and observed snow

1195 accumulation on the ground under the canopy for Umpqua, Oregon (OR) for water year 1997-

1196 1998 and (c,d) for Swamp Angel, Senator Beck, Colorado (CO) for water year 2008-2009.

1197 Columns refer to unloading schemes, while colors refer to loading configurations. Warmer

1198 colors representing interception schemes with greater interception amounts at warmer

1199 temperatures. Snow accumulation (Σ +ΔSWE) is represented by the cumulative sum of SWE

1200 increases, available for the Oregon site from a weighing lysimeter. Actual SWE is shown for the

1201 Colorado site, which, because little melt occurred during this period, matches well with modeled

1202 cumulative SWE in the open.

1203

1204 **Figure 6.** Intercepted snow (a) and temperature (b) for 1997-1998 at Umpqua, Oregon and (c,d)

1205 for 2008-2009 at Senator Beck, Colorado (subset of time-periods shown in Fig. 5), where

1206 colored lines refer to the loading schemes as in Section 3, and line styles represent variations in

1207 canopy unloading. Model parameters are for baseline simulations in Table 2. Black lines (a)

1208 show intercepted snow from a Ponderosa Pine tree cut and weighed on a lysimeter.

1209

1210 **Figure 7.** Cumulative losses of snow water equivalent from the canopy for (a) Umpqua, Oregon

1211 and (b) Senator Beck Colorado, for the baseline simulation using the temperature-wind

1212 unloading parameterization and the loading scheme of $I_e=f(T_{air})$ and no I_{max}.

1213

1214 **Figure 8**. Temperature change sensitivity for (a,b) Umpqua, OR for year 1997-98 and for (c,d)

1215 Senator Beck, CO for year 2008-09 for multiple model configurations with regards to (a,c) the

1216 fraction of seasonal-total snow accumulating under the canopy compared to the open and (b,d)

1217 the fraction of time when snow is present in the canopy. For reference, observed mean

1218 temperature for Oregon was 0°C and for Colorado was -7°C, so in general, Oregon temperatures

1219 were cooled while Colorado temperatures were warmed to compare results assuming similar

1220 "mean temperatures. The fractions observed at the Oregon site are plotted at the observed mean

1221 temperature.

1222

1223 **Figure 9**. Fraction of snow below the canopy compared to the open, as in Figure 8, but

1224 specifying specific run values at mean December to March temperatures of -7°C (observed at the

1225   CO site) and at 0°C (observed at the Oregon site). The value observed at the Oregon site is

1226   marked with a horizontal dashed line in (b).